

ENM

Volume XVI

Enhanced Night Visibility Series: Phase III—Characterization of Experimental Objects

PUBLICATION NO. FHWA-HRT-04-147

DECEMBER 2005



U.S. Department of Transportation
Federal Highway Administration

Research, Development, and Technology
Turner-Fairbank Highway Research Center
6300 Georgetown Pike
McLean, VA 22101-2296

FOREWORD

The overall goal of the Federal Highway Administration's (FHWA) Visibility Research Program is to enhance the safety of road users through near-term improvements of the visibility on and along the roadway. The program also promotes the advancement of new practices and technologies to improve visibility on a cost-effective basis.

The following document provides a characterization of the experimental objects used in the evaluation of the performance of drivers during nighttime driving using visual headlamp technologies and visual headlamp technologies augmented with in-vehicle displays for near- and far-infrared sensors. The experimental objects were used in the Phase III efforts of the Enhanced Night Visibility (ENV) project, a comprehensive evaluation of evolving and proposed headlamp technologies. The individual studies within the overall project are documented in an 18-volume series of FHWA reports, of which this is Volume XVI. It is anticipated that the reader will select those volumes that provide information of specific interest.

This report will be of interest to headlamp designers, automobile manufacturers and consumers, third-party headlamp manufacturers, human factors engineers, and people involved in headlamp and roadway specifications.

Michael F. Trentacoste
Director, Office of Safety
Research and Development

Notice

This document is disseminated under the sponsorship of the U.S. Department of Transportation in the interest of information exchange. The U.S. Government assumes no liability for the use of the information contained in this document.

The U.S. Government does not endorse products or manufacturers. Trademarks or manufacturers' names appear in this report only because they are considered essential to the objective of the document.

Quality Assurance Statement

The Federal Highway Administration (FHWA) provides high-quality information to serve Government, industry, and the public in a manner that promotes public understanding. Standards and policies are used to ensure and maximize the quality, objectivity, utility, and integrity of its information. FHWA periodically reviews quality issues and adjusts its programs and processes to ensure continuous quality improvement.

TECHNICAL REPORT DOCUMENTATION PAGE

| | | | |
|---|--|--|-----------|
| 1. Report No. FHWA-HRT-04-147 | 2. Government Accession No. | 3. Recipient's Catalog No. | |
| 4. Title and Subtitle Enhanced Night Visibility Series, Volume XVI: Phase III—Characterization of Experimental Objects | | 5. Report Date December 2005 | |
| | | 6. Performing Organization Code: | |
| 7. Author(s) Ronald B. Gibbons, Chris Edwards, Santosh Gupta | | 8. Performing Organization Report No. | |
| 9. Performing Organization Name and Address Virginia Tech Transportation Institute 3500 Transportation Research Plaza Blacksburg, VA 24061 | | 10. Work Unit No. | |
| | | 11. Contract or Grant No. DTFH61-98-C-00049 | |
| 12. Sponsoring Agency Name and Address Office of Safety Research and Development Federal Highway Administration 6300 Georgetown Pike McLean, VA 22101-2296 | | 13. Type of Report and Period Covered Final Report | |
| | | 14. Sponsoring Agency Code HRDS-05 | |
| 15. Supplementary Notes Contracting Officer's Technical Representative (COTR): Carl Andersen, HRDS-05 | | | |
| 16. Abstract <p>The Enhanced Night Visibility (ENV) project is a series of experiments undertaken to investigate different visual enhancement systems (VES) for the nighttime driving task. The purpose of this characterization activity is to establish the photometric nature of the objects presented to the observer during the ENV Phase III studies, which assessed headlamp beam patterns as well as the influence of infrared (IR) technology on object detection. The photometric measurements of interest are the object luminance and the background luminance. Other calculated parameters were established such as object contrast with the background and object visibility level. The measurements were taken at the threshold of detection and calculated for three visible-light VESs and three IR VESs.</p> <p>For the visible-light VESs, the photometric data showed the influence of the headlamp distribution and the suitability of the various metrics to predict object visibility. For the IR systems, the data gave an indication of the usage of the in-vehicle systems and their distraction level for the driver.</p> | | | |
| 17. Key Words Halogen, Headlamps, High Intensity Discharge, Infrared, Visibility, Vision Enhancement System, Photometry, Infrared, Characterization | | 18. Distribution Statement No restrictions. This document is available through the National Technical Information Service; Springfield, VA 22161. | |
| 19. Security Classif. (of this report) Unclassified | 20. Security Classif. (of this page) Unclassified | 21. No. of Pages 69 | 22. Price |

SI* (MODERN METRIC) CONVERSION FACTORS

APPROXIMATE CONVERSIONS TO SI UNITS

| Symbol | When You Know | Multiply By | To Find | Symbol |
|--|----------------------------|-----------------------------|-----------------------------|-------------------|
| LENGTH | | | | |
| in | inches | 25.4 | millimeters | mm |
| ft | feet | 0.305 | meters | m |
| yd | yards | 0.914 | meters | m |
| mi | miles | 1.61 | kilometers | km |
| AREA | | | | |
| in ² | square inches | 645.2 | square millimeters | mm ² |
| ft ² | square feet | 0.093 | square meters | m ² |
| yd ² | square yard | 0.836 | square meters | m ² |
| ac | acres | 0.405 | hectares | ha |
| mi ² | square miles | 2.59 | square kilometers | km ² |
| VOLUME | | | | |
| fl oz | fluid ounces | 29.57 | milliliters | mL |
| gal | gallons | 3.785 | liters | L |
| ft ³ | cubic feet | 0.028 | cubic meters | m ³ |
| yd ³ | cubic yards | 0.765 | cubic meters | m ³ |
| NOTE: volumes greater than 1000 L shall be shown in m ³ | | | | |
| MASS | | | | |
| oz | ounces | 28.35 | grams | g |
| lb | pounds | 0.454 | kilograms | kg |
| T | short tons (2000 lb) | 0.907 | megagrams (or "metric ton") | Mg (or "t") |
| TEMPERATURE (exact degrees) | | | | |
| °F | Fahrenheit | 5 (F-32)/9 or (F-32)/1.8 | Celsius | °C |
| ILLUMINATION | | | | |
| fc | foot-candles | 10.76 | lux | lx |
| fl | foot-Lamberts | 3.426 | candela/m ² | cd/m ² |
| FORCE and PRESSURE or STRESS | | | | |
| lbf | poundforce | 4.45 | newtons | N |
| lbf/in ² | poundforce per square inch | 6.89 | kilopascals | kPa |

APPROXIMATE CONVERSIONS FROM SI UNITS

| Symbol | When You Know | Multiply By | To Find | Symbol |
|-------------------------------------|-----------------------------|-------------|----------------------------|---------------------|
| LENGTH | | | | |
| mm | millimeters | 0.039 | inches | in |
| m | meters | 3.28 | feet | ft |
| m | meters | 1.09 | yards | yd |
| km | kilometers | 0.621 | miles | mi |
| AREA | | | | |
| mm ² | square millimeters | 0.0016 | square inches | in ² |
| m ² | square meters | 10.764 | square feet | ft ² |
| m ² | square meters | 1.195 | square yards | yd ² |
| ha | hectares | 2.47 | acres | ac |
| km ² | square kilometers | 0.386 | square miles | mi ² |
| VOLUME | | | | |
| mL | milliliters | 0.034 | fluid ounces | fl oz |
| L | liters | 0.264 | gallons | gal |
| m ³ | cubic meters | 35.314 | cubic feet | ft ³ |
| m ³ | cubic meters | 1.307 | cubic yards | yd ³ |
| MASS | | | | |
| g | grams | 0.035 | ounces | oz |
| kg | kilograms | 2.202 | pounds | lb |
| Mg (or "t") | megagrams (or "metric ton") | 1.103 | short tons (2000 lb) | T |
| TEMPERATURE (exact degrees) | | | | |
| °C | Celsius | 1.8C+32 | Fahrenheit | °F |
| ILLUMINATION | | | | |
| lx | lux | 0.0929 | foot-candles | fc |
| cd/m ² | candela/m ² | 0.2919 | foot-Lamberts | fl |
| FORCE and PRESSURE or STRESS | | | | |
| N | newtons | 0.225 | poundforce | lbf |
| kPa | kilopascals | 0.145 | poundforce per square inch | lbf/in ² |

*SI is the symbol for the International System of Units. Appropriate rounding should be made to comply with Section 4 of ASTM E380.

(Revised March 2003)

ENHANCED NIGHT VISIBILITY PROJECT REPORT SERIES

This volume is the 16th of 18 volumes in this research report series. Each volume is a different study or summary, and any reference to a report volume in this series will be referenced in the text as “ENV Volume I,” “ENV Volume II,” and so forth. A list of the report volumes follows:

| Volume | Title | Report Number |
|---------------|--|----------------------|
| I | Enhanced Night Visibility Series: Executive Summary | FHWA-HRT-04-132 |
| II | Enhanced Night Visibility Series: Overview of Phase I and Development of Phase II Experimental Plan | FHWA-HRT-04-133 |
| III | Enhanced Night Visibility Series: Phase II—Study 1: Visual Performance During Nighttime Driving in Clear Weather | FHWA-HRT-04-134 |
| IV | Enhanced Night Visibility Series: Phase II—Study 2: Visual Performance During Nighttime Driving in Rain | FHWA-HRT-04-135 |
| V | Enhanced Night Visibility Series: Phase II—Study 3: Visual Performance During Nighttime Driving in Snow | FHWA-HRT-04-136 |
| VI | Enhanced Night Visibility Series: Phase II—Study 4: Visual Performance During Nighttime Driving in Fog | FHWA-HRT-04-137 |
| VII | Enhanced Night Visibility Series: Phase II—Study 5: Evaluation of Discomfort Glare During Nighttime Driving in Clear Weather | FHWA-HRT-04-138 |
| VIII | Enhanced Night Visibility Series: Phase II—Study 6: Detection of Pavement Markings During Nighttime Driving in Clear Weather | FHWA-HRT-04-139 |
| IX | Enhanced Night Visibility Series: Phase II—Characterization of Experimental Objects | FHWA-HRT-04-140 |
| X | Enhanced Night Visibility Series: Phase II—Visual Performance Simulation Software for Objects and Traffic Control Devices | FHWA-HRT-04-141 |
| XI | Enhanced Night Visibility Series: Phase II—Cost-Benefit Analysis | FHWA-HRT-04-142 |
| XII | Enhanced Night Visibility Series: Overview of Phase II and Development of Phase III Experimental Plan | FHWA-HRT-04-143 |
| XIII | Enhanced Night Visibility Series: Phase III—Study 1: Comparison of Near Infrared, Far Infrared, High Intensity Discharge, and Halogen Headlamps on Object Detection in Nighttime Clear Weather | FHWA-HRT-04-144 |
| XIV | Enhanced Night Visibility Series: Phase III—Study 2: Comparison of Near Infrared, Far Infrared, and Halogen Headlamps on Object Detection in Nighttime Rain | FHWA-HRT-04-145 |
| XV | Enhanced Night Visibility Series: Phase III—Study 3: Influence of Beam Characteristics on Discomfort and Disability Glare | FHWA-HRT-04-146 |
| XVI | Enhanced Night Visibility Series: Phase III—Characterization of Experimental Objects | FHWA-HRT-04-147 |
| XVII | Enhanced Night Visibility Series: Phases II and III—Characterization of Experimental Vision Enhancement Systems | FHWA-HRT-04-148 |
| XVIII | Enhanced Night Visibility Series: Overview of Phase III | FHWA-HRT-04-149 |

TABLE OF CONTENTS

| | |
|---|----|
| CHAPTER 1—INTRODUCTION | 1 |
| CHAPTER 2—METHODS | 3 |
| EXPERIMENTAL DESIGN | 3 |
| Independent Variables..... | 4 |
| Dependent Variables..... | 14 |
| APPARATUS AND MATERIALS | 14 |
| CCD Photometer | 14 |
| Headlamp and IR System Alignment..... | 16 |
| Smart Road..... | 17 |
| MEASUREMENT PROCEDURE | 17 |
| DATA ANALYSIS | 18 |
| Calculated Variables..... | 19 |
| Object and VES Classification..... | 21 |
| Photometric Measurement Comparisons | 22 |
| Identifying the System Usage..... | 22 |
| Age Analysis | 22 |
| CHAPTER 3—RESULTS | 23 |
| VISIBLE SYSTEMS SUMMARY OF IR CLEAR RESULTS | 23 |
| PHOTOMETRIC ANALYSIS | 24 |
| Comparison of Detection and Recognition Values | 24 |
| Pedestrian Object Group | 27 |
| VIS Headlamp and Obstacle Object Group Analysis | 34 |
| VIS Headlamp and Retroreflective Object Group Analysis..... | 38 |
| Photometric Analysis Summary | 47 |
| IR SYSTEM USAGE | 47 |
| IR System Usage for Pedestrian Objects | 48 |
| IR System Usage for Obstacle Objects..... | 50 |
| IR System Usage for Retroreflective Objects..... | 51 |
| IR System Usage Summary..... | 54 |
| AGE ANALYSIS | 54 |
| CHAPTER 4—DISCUSSION | 57 |
| REFERENCES | 59 |

LIST OF FIGURES

| | |
|---|----|
| 1. Diagram. Bird's-eye view of HID 1 beam pattern. | 5 |
| 2. Diagram. Forward beam pattern of HID 1. | 5 |
| 3. Diagram. Bird's-eye view of HID 2 beam pattern. | 6 |
| 4. Diagram. Forward beam pattern of HID 2. | 6 |
| 5. Photo. Object: pedestrian, black clothing, left (BlackLF). | 8 |
| 6. Photo. Object: pedestrian, black clothing, right (BlackRT). | 8 |
| 7. Photo. Object: pedestrian, denim clothing, left (BlueLF). | 8 |
| 8. Photo. Object: pedestrian, denim clothing, right (BlueRT). | 9 |
| 9. Photo. Object: pedestrian in left turn, left side (LFtrnLF). | 9 |
| 10. Photo. Object: pedestrian in left turn, right side (LFtrnRT). | 9 |
| 11. Photo. Object: pedestrian in right turn, left side (RTtrnLF). | 10 |
| 12. Photo. Object: pedestrian in right turn, right side (RTtrnRT). | 10 |
| 13. Photo. Object: far off axis, left (FOALT). | 10 |
| 14. Photo. Object: far off axis, right (FOART). | 11 |
| 15. Photo. Object: bloom object, left (BloomLF). | 11 |
| 16. Photo. Object: bloom object, right (BloomRT). | 11 |
| 17. Photo. Object: dog. | 12 |
| 18. Photo. Object: pavement marking turn arrow. | 12 |
| 19. Photo. Object: raised retroreflective pavement markers. | 12 |
| 20. Photo. Object: sign. | 13 |
| 21. Photo. Object: tire tread. | 13 |
| 22. Photo. Measurement regions for pedestrians. | 14 |
| 23. Photo. Measurement regions for the tire tread. | 14 |
| 24. Photo. CCD photometer in experimental vehicle, side view. | 15 |
| 25. Photo. CCD photometer in experimental vehicle, front view. | 15 |
| 26. Photo. Headlamp testing rack. | 16 |
| 27. Diagram. Locations of objects in experiment. | 17 |
| 28. Equation. Contrast calculation. | 19 |
| 29. Equation. Basic ΔL_{th} calculation. | 19 |
| 30. Equation. Time factor calculation. | 20 |
| 31. Equation. Age factor calculation. | 20 |

| | |
|--|----|
| 32. Equation. Complete ΔL_{th} model calculation..... | 20 |
| 33. Equation. Visibility level calculation..... | 21 |
| 34. Bar graph. Comparison of object luminance at detection and recognition of pedestrian objects..... | 25 |
| 35. Bar graph. Comparison of object luminance at detection and recognition of retroreflective objects. | 26 |
| 36. Bar graph. Comparison of object luminance at detection and recognition of obstacle objects..... | 27 |
| 37. Bar graph. Mean luminance values at pedestrian object detection. | 28 |
| 38. Bar graph. Mean background luminance values at pedestrian object detection..... | 30 |
| 39. Bar graph. Mean contrast values at pedestrian object detection. | 31 |
| 40. Bar graph. Older driver mean visibility levels at pedestrian object detection..... | 32 |
| 41. Picture. Right turn right pedestrian in HID 2 condition..... | 33 |
| 42. Picture. Right turn right pedestrian in HLB condition..... | 33 |
| 43. Bar graph. Mean luminance values at obstacle object detection..... | 34 |
| 44. Bar graph. Mean background luminance values at obstacle object detection..... | 35 |
| 45. Bar graph. Mean contrast values at obstacle object detection. | 36 |
| 46. Bar graph. Older driver mean visibility levels at obstacle object detection..... | 37 |
| 47. Bar graph. Mean luminance values at retroreflective object detection..... | 39 |
| 48. Bar graph. Mean luminance values at retroreflective object recognition. | 40 |
| 49. Bar graph. Mean background luminance values at retroreflective object detection. | 41 |
| 50. Bar graph. Mean background luminance values at retroreflective object recognition. | 42 |
| 51. Bar graph. Mean contrast values at retroreflective object detection..... | 43 |
| 52. Bar graph. Mean contrast values at retroreflective object recognition..... | 44 |
| 53. Bar graph. Older driver mean visibility levels at retroreflective object detection. | 45 |
| 54. Bar graph. Older driver mean visibility levels at retroreflective object recognition. | 46 |
| 55. Bar graph. Comparison of older driver mean visibility levels at pedestrian object detection with the IR system versus the VIS systems. | 49 |
| 56. Bar graph. Comparison of older driver mean visibility levels at obstacle object detection with the IR systems versus the VIS systems..... | 50 |
| 57. Bar graph. Comparison of older driver mean visibility levels at retroreflective object detection with the IR systems versus the VIS systems..... | 52 |
| 58. Bar graph. Comparison of older driver mean visibility levels at sign recognition for the IR systems versus the VIS systems..... | 53 |
| 59. Line graph. Age comparison for detection of pedestrians. | 55 |

LIST OF TABLES

| | |
|---|-----------|
| 1. VES type used in the experiment..... | 3 |
| 2. Objects used in the experiment..... | 3 |
| 3. VES configurations and properties. | 7 |
| 4. Object descriptions. | 8 |
| 5. Object dimension summarization..... | 21 |
| 6. VIS systems corresponding to minimum and maximum VIS system distances for detection and recognition. | 23 |
| 7. Pearson-r correlation results between detection and recognition by data and object type. | 24 |
| 8. IR systems corresponding to minimum and maximum IR distances for detection and recognition. | 48 |

LIST OF ACRONYMS AND ABBREVIATIONS

General Terms

| | |
|---------|---|
| CCD | charged coupled device |
| ENV | Enhanced Night Visibility |
| HHD | high head down |
| SUV | sport utility vehicle |
| VES | vision enhancement system |
| IR | infrared |
| far IR | portion of electromagnetic spectrum from 2.5 micrometers (μm) to 350 μm |
| N | sample size |
| near IR | portion of electromagnetic spectrum from 700 nanometers to 5 μm |
| FOV | field of view |
| VIS | visible light |

Vision Enhancement Systems

| | |
|-------|---|
| FIR | far infrared vision system |
| HID 1 | high intensity discharge (narrow beam distribution) |
| HID 2 | high intensity discharge (wide beam distribution) |
| HLB | halogen (i.e., tungsten-halogen) low beam |
| NIR | near infrared vision system |

Objects

| | |
|---------|---|
| BlackLF | pedestrian, black clothing, left |
| BlackRT | pedestrian, black clothing, right |
| BloomLF | bloom object, left (denim clothing) |
| BloomRT | bloom object, right (denim clothing) |
| BlueLF | pedestrian, denim clothing, left |
| BlueRT | pedestrian, denim clothing, right |
| FOALT | far off axis left (denim clothing) |
| FOART | far off axis right (denim clothing) |
| LFtrnLF | pedestrian in left turn, left side (denim clothing) |
| LFtrnRT | pedestrian in left turn, right side (denim clothing) |
| RRPM | raised retroreflective pavement marker |
| RTtrnLF | pedestrian in right turn, left side (denim clothing) |
| RTtrnRT | pedestrian in right turn, right side (denim clothing) |

Measurements

| | |
|------------------------|--------------------------------|
| ΔL | luminance difference |
| ΔL_{th} | threshold luminance difference |
| C | contrast |

cd/m² candela per square meter
cm centimeters
ft feet
fL footlamberts
m meters
mi/h miles per hour
mm millimeters
s seconds
VL visibility level

Calculated Variables

AF age factor
F_{CP} negative contrast factor
L luminance
t observation time
TF time factor

CHAPTER 1—INTRODUCTION

This project is a follow-on analysis to the study reported in Enhanced Night Visibility (ENV) Volume XIII, Phase III—Study 1: *Comparison of Near Infrared, Far Infrared, High Intensity Discharge, and Halogen Headlamps on Object Detection in Nighttime Clear Weather* (referred to as the IR Clear study). The IR Clear study evaluated six different automotive vision enhancement systems (VESs). Three of these were infrared (IR) systems, of which two were active near-IR systems, and the third was a passive far-IR system. The remaining three VESs were visible-light (VIS) systems; one was a standard halogen (i.e., tungsten-halogen) system used in previous ENV experiments, and two were high intensity discharge (HID) systems, each with a different beam distribution. In the basic experiment, the visibility of pedestrians, simulated animals, tire treads, and roadway infrastructure (e.g., signs and pavement markers) was tested with each of the VESs.

This follow-on investigation measured the photometric characteristics of the objects used in the experiment. The measurements were made using a charged coupled device (CCD) photometer with each of the VESs. The luminance of each object and the background behind it were derived from the photometric data. Then these values were used to model the contrast and visibility level of the object at the threshold of visibility.

The purpose of this investigation is to use the measured data as a tool to evaluate the capability of the VESs to provide adequate visibility of objects in the roadway. The photometric analysis provided insight into the performance of the VIS systems; however, it should be noted that the photometric analysis provided only a method of identifying the usage of the IR systems and not their photometric characteristics.

The following research questions for this project were drawn from the results of the IR Clear study documented in ENV Volume XIII:

- Is there a relationship between measured data or calculated values and the visibility distance?
- Because all of the photometric measurements are made at threshold of visibility, are the resulting contrast or visibility levels similar?

- When does an IR system appear to be used by the driver?
- Does having an IR system in the vehicle require higher object contrast and visibility levels at threshold than when the system is not used?
- What is the effect of beam pattern on the visibility of the objects?

CHAPTER 2—METHODS

EXPERIMENTAL DESIGN

This study was a 6 by 17 design with two independent variables: VES configuration and type of object. Six types of VESs were tested, of which, three were VIS systems and three were IR-based systems with high head down (HHD) displays. Ten different objects were tested in different positions on the road, generating 17 different object and position combinations. Table 1 presents the VES categories, and table 2 includes the object categories. The VESs and objects are described in more detail in the Independent Variables section.

Table 1. VES type used in the experiment.

| VES Type | VES Configuration | VES Abbreviation |
|----------|---|------------------|
| VIS | High intensity discharge (narrow beam distribution) | HID 1 |
| VIS | High intensity discharge (wide beam distribution) | HID 2 |
| VIS | Halogen (i.e., tungsten-halogen) | HLB |
| IR | Passive far IR | FIR |
| IR | Laser-based active near IR | NIR 1 |
| IR | Halogen-based active near IR | NIR 2 |

Table 2. Objects used in the experiment.

| | Object | Abbreviation |
|------------------------------|---|--------------|
| Pedestrian Group | Pedestrian, Black Clothing, Left | BlackLF |
| | Pedestrian, Black Clothing, Right | BlackRT |
| | Pedestrian, Denim Clothing, Left | BlueLF |
| | Pedestrian, Denim Clothing, Right | BlueRT |
| | Pedestrian in Left Turn, Left Side (Denim Clothing) | LFtrnLF |
| | Pedestrian in Left Turn, Right Side (Denim Clothing) | LFtrnRT |
| | Pedestrian in Right Turn, Left Side (Denim Clothing) | RTtrnLF |
| | Pedestrian in Right Turn, Right Side (Denim Clothing) | RTtrnRT |
| | Far Off Axis Left (Denim Clothing) | FOALT |
| | Far Off Axis Right (Denim Clothing) | FOART |
| | Bloom Object, Left (Denim Clothing) | BloomLF |
| | Bloom Object, Right (Denim Clothing) | BloomRT |
| Retroreflective Group | Raised Retroreflective Pavement Marker | RRPM |
| | Sign | Sign |
| | Turn Arrow | Arrow |
| Obstacle Group | Dog | Dog |
| | Tire Tread | Tire Tread |

The dependent variables in the design of this experiment were based on photometric measurements of the objects. The measurements were performed at the mean detection and recognition distances found in the initial experiment. The photometric measurements of object luminance and background luminance were used to calculate values for contrast and visibility level for each VES and object scenario. A detailed explanation of the measurement and calculation of these four variables (the dependent variables for this study) is provided in the Dependent Variables section.

Independent Variables

The independent variables for this experiment, VES configuration and type of object, are described in more detail below.

VES Types

For this experiment, each VIS system was comprised of two headlamps mounted on one of the four experimental vehicles. The IR systems were comprised of two headlamps, a detector system, a viewing screen, and emitters for the active near IR systems.

Prototype Far Infrared Vision System: A prototype far infrared (FIR) vision system was tested on a sport utility vehicle (SUV). The system display used a directly reflected virtual image with an 11.7° horizontal by 4° vertical field of view (FOV). The reflective mirror, located in an HHD position on centerline with the driver, was mounted directly on the instrument panel surface above the instrument cluster. The reported magnification at the eye was approximately 1:1. The headlamps used were the production halogen headlamps for this vehicle.

Prototype Near Infrared Vision System 1: A prototype near infrared (NIR 1) vision system that used a laser IR emitter was tested on a second SUV. The system used a curved mirror display with an 18° horizontal by approximately 6° vertical FOV. The mirror, located in an HHD position on centerline with the driver, was placed directly on the instrument panel surface above the instrument cluster. The reported magnification at the eye was approximately 2:3. The headlamps used were the production halogen headlamps for this vehicle.

Prototype Near Infrared Vision System 2: A prototype near infrared (NIR 2) system that used broadband halogen IR emitters was tested on the same type of SUV as the FIR system. The system display used a directly reflected virtual image with an 11.7° horizontal by 4° vertical field of view. The reflective mirror, located in an HHD position on centerline with the driver, was placed directly on the instrument panel surface above the instrument cluster. The reported magnification at the eye was approximately 1:1. The headlamps used were the production halogen headlamps for this vehicle.

HID 1: The HID 1 headlamps were tested on a third SUV style. The headlamps were mounted on a light rack system that was placed on the front of the vehicle. The Apparatus and Materials section gives a further description of the mounting process. These headlamps have a narrower lighting footprint than the other HID headlamps tested in this study (figure 1 and figure 2).

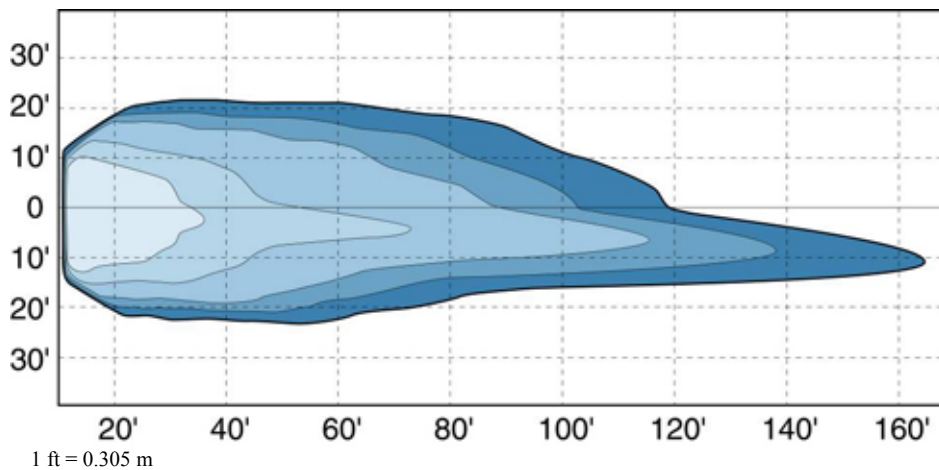


Figure 1. Diagram. Bird's-eye view of HID 1 beam pattern.

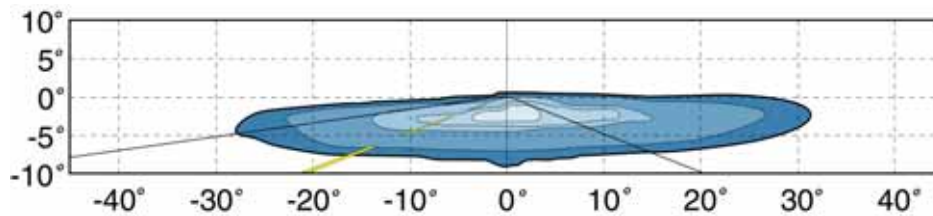


Figure 2. Diagram. Forward beam pattern of HID 1.

HID 2: The HID 2 headlamps were tested on a similar SUV as that outfitted with the HID 1 headlamps. The HID 2 headlamps were mounted on a light rack system placed on the front of the

vehicle. The HID 2 headlamps have a wider lighting footprint than the HID 1 headlamps. Figure 3 and figure 4 show the HID 2 headlamp beam pattern.

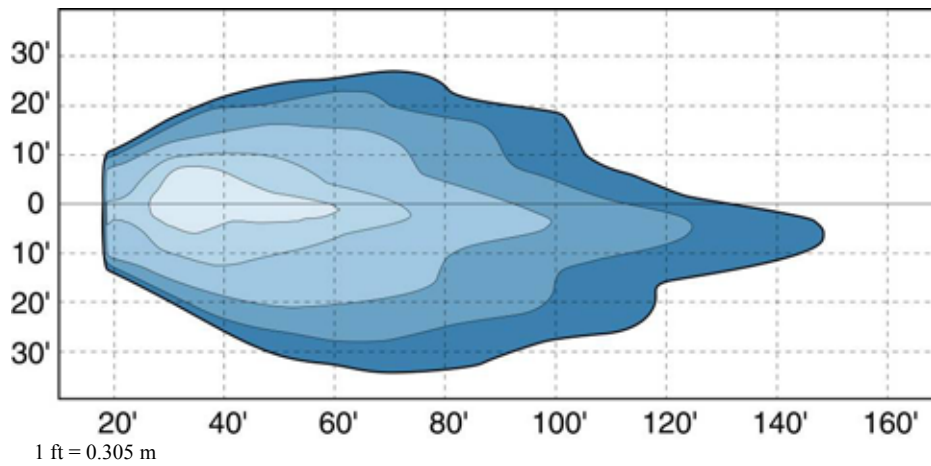


Figure 3. Diagram. Bird's-eye view of HID 2 beam pattern.

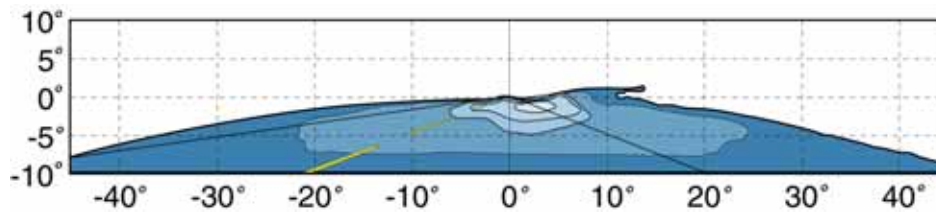


Figure 4. Diagram. Forward beam pattern of HID 2.

HLB: The halogen low beam headlamps were tested on the same make of SUV used to test the HID systems. A light rack was used to attach the headlamps to the front of the vehicle. These headlamps were tested to provide a benchmark within this experiment and for comparison to the other VESs tested throughout the various studies in the ENV project.

VES Summary: Table 3 shows the different VESs; the vehicles on which the VESs were tested; the headlamps on the vehicle; and, where applicable, the HID system pattern description or the display method, FOV, and image size. Specification of displays, display FOVs, and image sizes were provided by the system engineers responsible for the systems. ENV Volume XVII, *Characterization of Experimental Vision Enhancement Systems*, provides an indepth look at the technical specifications of each headlamp.

Table 3. VES configurations and properties.

| Tested Technology | VES Abbreviation | Test Vehicle | Headlamps | Display | Display FOV | Image Size |
|-------------------------------|------------------|--------------|------------------------|------------------------------|-------------|--------------------------|
| HLB headlamps | HLB | SUV 3 | tested HLB | none | n/a | n/a |
| HID headlamps | HID 1 | SUV 3 | tested HID 1 | none | n/a | n/a |
| HID headlamps | HID 2 | SUV 3 | tested HID 2 | none | n/a | n/a |
| Far IR | FIR | SUV 1 | SUV 1 manufacturer HLB | direct reflect virtual image | 11.7° by 4° | ~1:1 |
| Near IR with laser emitter | NIR 1 | SUV 2 | SUV 2 manufacturer HLB | curved mirror virtual image | 18° by ~6° | minification ~2:3 actual |
| Near IR with halogen emitters | NIR 2 | SUV 1 | SUV 1 manufacturer HLB | direct reflect virtual image | 11.7° by 4° | ~1:1 |

Again, it should be noted that although the display characteristics of the IR systems are provided, they were not tested as part of this object characterization activity. The performance of the headlamps associated with the IR systems and the visual response to them was evaluated.

Objects

The IR Clear study measured the detection and recognition distances of the 10 different objects for each of the VESs. Some objects appeared on the right side of the road, the left side of the road, or in the center of the road, for a total of 17 different combinations of object and position. The objects selected for this study were grouped into three sets: pedestrians, retroreflective objects, and obstacles. The objects were the same as those used in the IR Clear experiment, and they are described in more detail in ENV Volume XIII.

One of the IR Clear study’s tested objects was a bloom scenario, which represented a pedestrian behind an approaching vehicle. The purpose of that test was to evaluate the performance of the IR systems in the presence of glare. For this object characterization activity, the bloom scenario excluded the opposing headlamps and measured only the luminance of the pedestrian. Table 4 and figure 5 through figure 21 describe the objects used for the study as well as their locations. Note that the photographs were taken during daylight hours to demonstrate more clearly the appearance and position of the objects.

Table 4. Object descriptions.




| Object Description | Objects |
|---|---|
| <p>Pedestrian wearing black scrubs stood on the left side of the road as viewed from the experimental vehicle. Pedestrian stood 30.5 cm (12 inches) outside the far lane boundary on a straight segment of roadway. Pedestrian stood with arms down to the side and faced the oncoming test vehicle.</p> |  <p>Figure 5. Photo. Object: pedestrian, black clothing, left (BlackLF).</p> |
| <p>Pedestrian wearing black scrubs stood on the right side of the road as viewed from the experimental vehicle. Pedestrian stood 30.5 cm (12 inches) to the right of the experimental vehicle's right-hand lane boundary on a straight segment of roadway. Pedestrian stood with arms down to the side and faced the oncoming test vehicle.</p> |  <p>Figure 6. Photo. Object: pedestrian, black clothing, right (BlackRT).</p> |
| <p>Pedestrian wearing blue denim scrubs stood on the left side of the road, as viewed from the experimental vehicle. Pedestrian stood 30.5 cm (12 inches) outside the far lane boundary on a straight segment of roadway. Pedestrian stood with arms down to the side and faced the oncoming test vehicle.</p> |  <p>Figure 7. Photo. Object: pedestrian, denim clothing, left (BlueLF).</p> |

Table 4. Object descriptions. (continued)




| Object Description | Objects |
|--|---|
| <p>Pedestrian wearing blue denim scrubs stood on the right side of the road as viewed from the experimental vehicle. Pedestrian stood 30.5 cm (12 inches) to the right of the experimental vehicle's right-hand lane boundary on a straight segment of roadway. Pedestrian stood with arms down to the side and faced the oncoming test vehicle.</p> |  <p>Figure 8. Photo. Object: pedestrian, denim clothing, right (BlueRT).</p> |
| <p>In a 1,250-m radius left-hand curve, a pedestrian wearing blue denim scrubs stood on the left side of the road as viewed from the experimental vehicle. Pedestrian stood 30.5 cm (12 inches) outside the far lane boundary. Pedestrian stood with arms down to the side and faced the oncoming test vehicle.</p> |  <p>Figure 9. Photo. Object: pedestrian in left turn, left side (LFtrnLF).</p> |
| <p>In a 1,250-m radius left-hand curve, a pedestrian wearing blue denim scrubs stood on the right side of the road as viewed from the experimental vehicle. Pedestrian stood 30.5 cm (12 inches) to the right of the experimental vehicle's right-hand lane boundary. Pedestrian stood with arms down to the side and faced the oncoming test vehicle.</p> |  <p>Figure 10. Photo. Object: pedestrian in left turn, right side (LFtrnRT).</p> |

Table 4. Object descriptions. (continued)




| Object Description | Objects |
|---|---|
| <p>In a 1,250-m radius right-hand curve, a pedestrian wearing blue denim scrubs stood on the left side of the road as viewed from the experimental vehicle. Pedestrian stood 30.5 cm (12 inches) outside the far lane boundary. Pedestrian stood with arms down to the side and faced the oncoming test vehicle.</p> |  <p>Figure 11. Photo. Object: pedestrian in right turn, left side (RTtrnLF).</p> |
| <p>In a 1,250-m radius right-hand curve, a pedestrian wearing blue denim scrubs stood on the right side of the road as viewed from the experimental vehicle. Pedestrian stood 30.5 cm (12 inches) to the right of the experimental vehicle's right-hand lane boundary. Pedestrian stood with arms down to the side and faced the oncoming test vehicle.</p> |  <p>Figure 12. Photo. Object: pedestrian in right turn, right side (RTtrnRT).</p> |
| <p>Pedestrian wearing blue denim scrubs stood on the left side of the road as viewed from the experimental vehicle. Pedestrian stood 9.5 m (31 ft) to the left of the center of the experimental vehicle's lane of travel. Pedestrian stood with arms down to the side and faced the oncoming test vehicle.</p> |  <p>Figure 13. Photo. Object: far off axis, left (FOALT).</p> |

Table 4. Object descriptions. (continued)




| Object Description | Objects |
|--|---|
| <p>Pedestrian wearing blue denim scrubs stood on the right side of the road as viewed from the experimental vehicle. Pedestrian stood 9.5 m (31 ft) to the right of the center of the experimental vehicle's lane of travel. Pedestrian stood with arms down to the side and faced the oncoming test vehicle.</p> |  <p>Figure 14. Photo. Object: far off axis, right (FOART).</p> |
| <p>With a vehicle parked with its headlamps on in the oncoming lane, a pedestrian wearing blue denim scrubs stood on the left side of the road as viewed from the experimental vehicle. Pedestrian stood 30.5 cm (12 inches) outside the far lane boundary and in line with the rear wheels of the parked vehicle. Pedestrian stood with arms down to the side and faced the oncoming test vehicle.</p> |  <p>Figure 15. Photo. Object: bloom object, left (BloomLF).</p> |
| <p>With a vehicle parked with its headlamps on in the oncoming lane, a pedestrian wearing blue denim scrubs stood on the right side of the road as viewed from the experimental vehicle. Pedestrian stood 30.5 cm (12 inches) to the right of the experimental vehicle's right-hand lane boundary and in line with the rear wheels of the parked vehicle. Pedestrian stood with arms down to the side and faced the oncoming test vehicle.</p> |  <p>Figure 16. Photo. Object: bloom object, right (BloomRT).</p> |

Table 4. Object descriptions. (continued)






| Object Description | Objects |
|--|---|
| <p>The dog mockup was placed on the centerline that divides the two lanes; the dog's head faced the experimental vehicle's lane of travel. The dog had internal heating elements to warm the body. Surface temperature of the dog was 26.6–32.2 °C (80–90 °F).</p> |  <p>Figure 17. Photo. Object: dog.</p> |
| <p>A turn arrow made of retroreflective pavement tape was placed in the center of the experimental vehicle's lane of travel. The arrow was pointed either right or left.</p> |  <p>Figure 18. Photo. Object: pavement marking turn arrow.</p> |
| <p>Two RRPMs were placed on the road, one before and one after a skip mark. The RRPMs were placed with the white reflective side facing the oncoming test vehicle.</p> |  <p>Figure 19. Photo. Object: raised retroreflective pavement markers.</p> |

Table 4. Object descriptions. (continued)

| Object Description | Objects |
|---|--|
| <p>Signs were placed to the right of the experimental vehicle’s right-hand lane boundary. Signs were placed with the lower edge approximately 2.1 m (7 ft) above the pavement, with the planes of the signs perpendicular to the lane of travel. A 60.9-cm by 60.9-cm (24-inch by 24-inch) stop sign and a 60.9-cm by 91.4-cm (24-inch by 36-inch) “SPEED LIMIT 55” sign were presented beside each other. In another scenario, a 60.9-cm by 60.9-cm (24-inch by 24-inch) yield sign and a 60.9-cm by 91.4-cm (24-inch by 36-inch) “SPEED LIMIT 30” sign were presented beside each other. The number height on the speed limit signs was 25.7 cm (10 inches). Signs were mounted on wooden supports, which were painted matte black. Figure 20 shows yield and speed limit sign.</p> |  <p>Figure 20. Photo. Object: sign.</p> |
| <p>A tire tread was centered on the right boundary line of the experimental vehicle’s lane of travel. The tire was kept outside during the day to maintain it at realistic outdoor temperatures.</p> |  <p>Figure 21. Photo. Object: tire tread.</p> |

Dependent Variables

The dependent variables in this experiment are derived from the measured photometric images made by the CCD photometer. The first measurement is the object luminance, or mean luminance of the object in the image. The other measurements are the background luminance, or the mean of the background luminance from above, from below, and to either side of the object. The white outlines in figure 22 and figure 23 show the measurement regions for the pedestrians and tire tread scenarios, respectively.

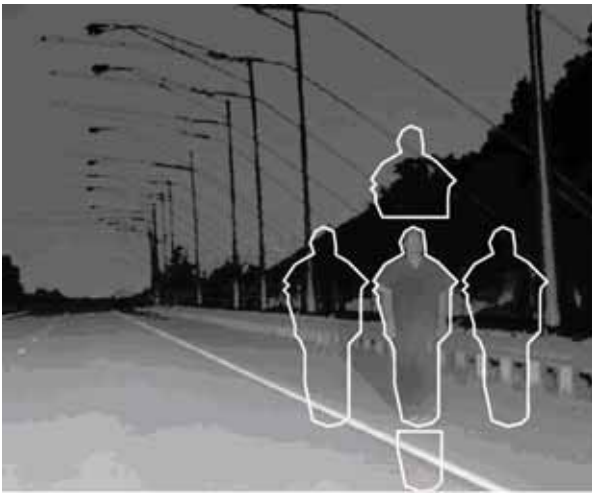


Figure 22. Photo. Measurement regions for pedestrians.



Figure 23. Photo. Measurement regions for the tire tread.

APPARATUS AND MATERIALS

CCD Photometer

As in the IR Clear study, the object characterization activity used five experimental vehicles, two mid-sized SUVs and three full-sized SUVs. The luminance was measured with a CCD photometer, which allows measurement of the average luminance of a surface. The CCD device was mounted in the driver's seat of the experimental vehicle. A 50-mm lens provided an image as close to the human visual system as possible. Figure 24 and figure 25 show the photometer and its locations in the experimental vehicle from the left and front side of the vehicle.



Figure 24. Photo. CCD photometer in experimental vehicle, side view.



Figure 25. Photo. CCD photometer in experimental vehicle, front view.

The output from this system allows for the characterization of the luminance of any point in the image.

Headlamp and IR System Alignment

The HID 1 headlamps, HID 2 headlamps, and HLB headlamps were mounted on a light bar on the front of two mid-sized SUVs during testing (figure 26). To change from one configuration to another, the HLB and HID headlamps were moved onto, off of, and between vehicles. Each light assembly movement required a re-aiming process, which took place before the experimental session started each night. At the beginning of the Phase II studies, a headlamp aimer was not available to the contractor, so an aiming protocol was developed with the help of experts in the field. (See references 1, 2, 3, and 4.) During the photometric characterization of the headlamps, it was discovered that the position of the maximum intensity location of the HLB system was aimed higher and more toward the left than typically specified. This aiming deviation likely influenced the visibility testing results in the IR Clear study; however, this object characterization activity reproduced that aiming deviation to evaluate the objects as they were presented to the experimental participants. ENV Volume XVII, *Characterization of Experimental Vision Enhancement Systems*, discusses the details of the aiming procedure and maximum intensity location.



Figure 26. Photo. Headlamp testing rack.

Smart Road

The Virginia Smart Road was used for the IR Clear study and the object characterization activity. Thirty-three locations were used to present objects, with some locations being used for left, right, or center presentation of objects. Some locations were acceptable for certain objects or for certain approach directions to achieve consistent ambient lighting and road geometry. Figure 27 presents a schematic of the Smart Road with examples of object locations. All of the object and location combinations that were used in the IR Clear study were used in this activity. The characterization of any one object was considered to be the mean of all the measurements from all the locations where the object appeared.

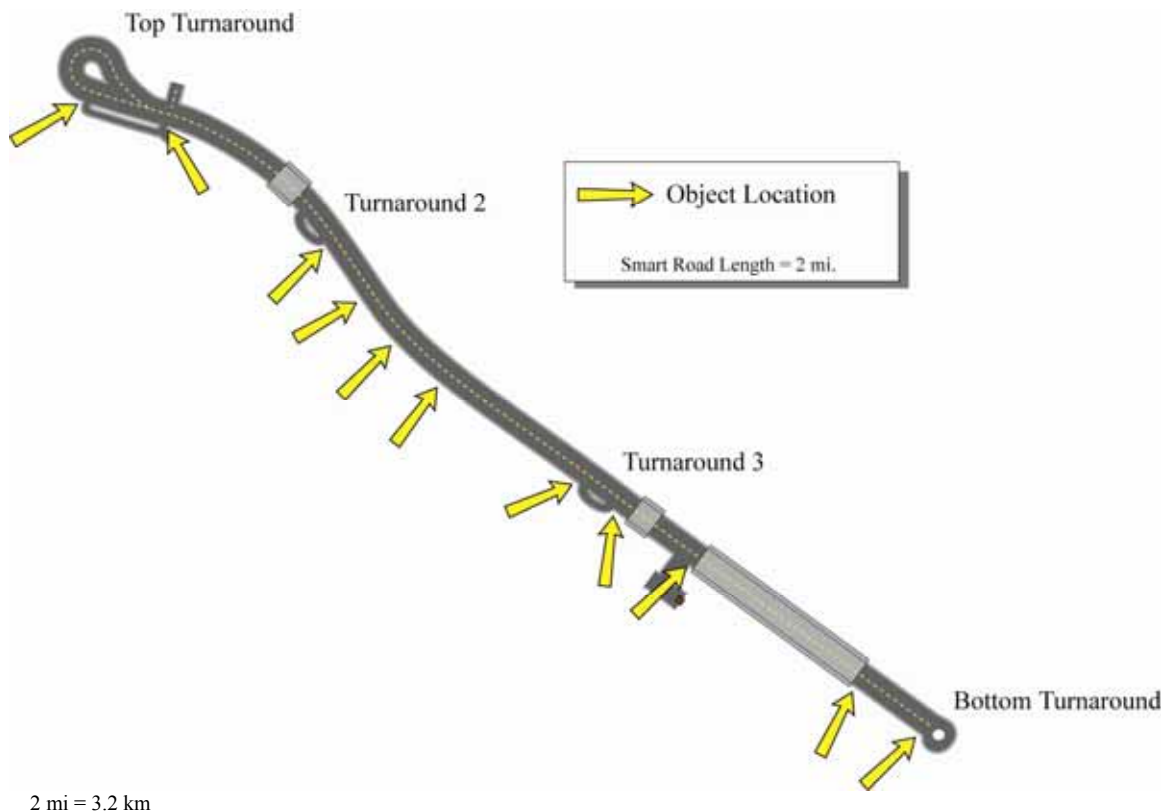


Figure 27. Diagram. Locations of objects in experiment.

MEASUREMENT PROCEDURE

The measurements were conducted in several nighttime sessions at the test facility. In each session, an experimental vehicle with the VES being evaluated was outfitted with the CCD photometer in the driver's seat. An experimenter, positioned in the driver's seat, was able to

operate the vehicle. A second experimenter, located in the passenger's seat, was responsible for the operation of the photometer software. For each condition, the driver, with the assistance of an onroad experimenter, placed the vehicle at the mean detection distance from the object being evaluated. A second onroad experimenter then simulated the pedestrian objects or placed the other objects in the appropriate location, and the photometric measurement was taken from the vehicle. After completion of the photometric measurement, the vehicle was moved to the location of the next object, and the process was repeated. This process was used for all VES, object type, and location combinations.

Software designed to operate the CCD photometer was used to obtain the luminance data of each object in each presentation location with all VESs. For each VES, a photometric file was created that could then be analyzed for the dependent variables. One image was taken at the previously determined mean detection distance and one at the mean recognition distance for each object. The software created an outline of the object. Using this traced shape, the luminance of the object and the luminance of its surrounding background regions (above, below, left, and right) were obtained. The background luminance measurements of the left or right regions were gathered by placing the traced shape of the object to the left or right of the target object. A similar procedure was used to measure the luminance of top and bottom background regions. The average luminance of the object itself was measured by highlighting around its edge. To determine luminance of different parts of the pedestrians, the software traced a shape that was only one-third of the pedestrian, from the knees down or the chest up. This shape was then used to gather the top and bottom luminance values. The measurements for all objects and all VESs were made with this system.

DATA ANALYSIS

An analysis of the results allows investigation of the effect of the visible-light VESs on the photometric data. Because the IR systems do not emit visible light, the photometric data were used to determine when detections were made at levels below the threshold of visibility, which would imply that the IR systems were used to detect the objects. Finally, an analysis of the participants' ages was included to compare the age results to the photometric results.

Calculated Variables

Using the photometric data of object luminance and background luminance, two other metrics were calculated—contrast and visibility level.

Contrast

The contrast of an object to its background is calculated based on the difference of the luminance of the object and the luminance of the background. Negative contrast occurs when the object is darker than the background. This relationship is shown in figure 28.

$$C = \frac{L_{Object} - L_{Background}}{L_{Background}}$$

Figure 28. Equation. Contrast calculation.

For the pedestrian objects, the contrast was evaluated using the mean of the background measurements and the mean of the object measurements.

Visibility Level

The visibility level was calculated based on the object visibility model of Adrian.⁽⁵⁾ In his model, the threshold luminance difference (ΔL_{th}) is defined as the difference of the luminance of the target and the luminance of the background that allows the observer to just detect the presence of the object. Adrian's model is defined for mesopic viewing conditions, which remove issues such as color differences and spectral sensitivity. The ΔL_{th} is calculated according to the model, and it is based on the size of the object and the background luminance, observation time, age of the observer, and polarity of the contrast.

The Adrian model is calculated using a basic formula with additions to modify the result for various conditions. The basic calculation is shown in figure 29.

$$\Delta L_{th} = k \left(\frac{\phi^2}{\alpha} + L^2 \right)^2$$

Figure 29. Equation. Basic ΔL_{th} calculation.

The functions Φ and L are both functions of the background luminance, and they are defined in Adrian's paper.⁽⁵⁾ The value of α is the angular size of the object in minutes of arc. The factor k is a constant, which scales the ΔL_{th} result to a probability factor. For 99.9 percent probability of detection, k would equal 2.6; for 50 percent probability of detection, k would equal 1.

This ΔL_{th} function is limited to 2 s of observation time. The general form of the time factor (TF) developed to account for shorter periods of time is shown in figure 30.

$$TF = \frac{a(\alpha, L_B) + t}{t}$$

Figure 30. Equation. Time factor calculation.

In this time factor equation, t represents the observation time, and a , which is defined in Adrian's paper,⁽⁵⁾ is a function of the target size and background luminance.

Objects that appear in negative contrast (object darker than background) are more easily seen than those that appear in positive contrast (object lighter than background). A factor (F_{CP}) was developed based on the target size and background luminance.

The final factor that must be accounted for is the age of the observer. The basic model is developed for a 23-year-old observer. To account for a different age group, the age factor (AF) equation shown in figure 31 must be used. The values of the constants a , b , and c are presented in Adrian's document.⁽⁵⁾

$$AF = \frac{(Age - a)^2}{b} + c$$

Figure 31. Equation. Age factor calculation.

The final model of the ΔL_{th} calculation is shown in the equation in figure 32.

$$\Delta L_{th} = k \left(\frac{\phi^2}{\alpha} + L^2 \right)^2 \cdot TF \cdot F_{CP} \cdot AF$$

Figure 32. Equation. Complete ΔL_{th} model calculation.

As a metric for visibility, VL is the ratio of the actual luminance difference and ΔL_{th} . The formula for this calculation is seen in figure 33, where C stands for contrast.

$$VL = \frac{\Delta L_{Actual}}{\Delta L_{Threshold}} = \frac{L_{Object} - L_{Background}}{\Delta L_{Threshold}} = \frac{C_{Actual}}{C_{Threshold}}$$

Figure 33. Equation. Visibility level calculation.

In this calculation, when the visibility level is 1 it implies a 50 percent probability of detection, thus the distance at which the VL equals 1 should be the mean detection distance. In a driving task, however, the practical threshold is higher to allow for driver distraction and workload. The Illuminating Engineering Society of North America RP-8 uses a visibility level of 2.6 to 3.8 in practice.⁽⁶⁾

The complete ΔL_{th} model was used to calculate the visibility level of all of the objects in the object characterization activity. For this calculation, the observation time was set to 0.2 s. The target size was calculated based on the angular size subtended by the target. The object dimensions used to calculate the threshold luminance differences are summarized in table 5.

Table 5. Object dimension summarization.

| Object | Height (ft) | Breadth (ft) | Length/Edge (ft) | Diameter (ft) |
|-------------|-------------|--------------|------------------|---------------|
| Pedestrians | 6.00 | 1.00 | | |
| Arrow | | 8.00 | 7.67 | |
| RRPMs | 0.05 | 0.35 | 0.29 | |
| Rec 30/55 | | 2.50 | 2.00 | |
| Stop Sign | 2.00 | | 0.83 | |
| Yield Sign | | | 2.75 | |
| Dog | 0.75 | 0.50 | 1.42 | |
| Tire | 0.75 | | | 2.25 |

1 ft = 0.305 m.

Object and VES Classification

As in the data analysis for the IR Clear study, the objects were divided into three groups: pedestrian, retroreflective object, and obstacle. The pedestrian group included all scenarios that involved detecting and recognizing a pedestrian, including the bloom scenario, both black- and denim-clothed pedestrians, pedestrians in turns, and far-off-axis pedestrians. The retroreflective object group included the turn arrow, the RRPMs, and the signs. The obstacle group included the

dog and the tire tread; these two objects were both smaller, low-contrast objects that extended into the lane of the participant vehicle. The VESs were also grouped into two categories: VIS systems, including the HLB and HID headlamps, and infrared systems, including the FIR and NIR systems.

Photometric Measurement Comparisons

An assessment of the means of the data for VIS systems with respect to luminance, background luminance, contrast, and visibility levels was conducted to identify potential differences between each system type. It was thought that a statistical comparison was not an appropriate method of analysis at this juncture, and thus a confidence interval of the means for VES and object type was created for each of the photometric measurements. It should be noted that if the objects were measured only once for each VES and object combination, it meant that an object appeared on the road in only one location, and no estimate of the measurement error could be obtained.

Identifying the System Usage

The process of detecting objects in the roadway when using an IR system is not direct visual observation of the object. As discussed, the IR systems use a camera sensitive to portions of the electromagnetic spectrum other than the visual region and create a visual representation of the detector response on an in-vehicle display. The photometric data were used as a means to indicate use of the IR systems' in-vehicle display by the study participants. If the calculated visibility level for an object at the mean detection distance was significantly less for the IR system than the visibility level at detection when using a VIS system, then it was assumed that the IR system was used, and the object was not detected by direct observation through the windshield.

Age Analysis

The final aspect of interest in this analysis is the effect of age. Using the age factor associated with the visibility-level model identified earlier, the age factor results from the IR Clear study were compared to the modeled results. The ratio of the performance by older drivers to that of younger drivers was then compared to an equivalent ratio calculated from the model.

CHAPTER 3—RESULTS

The results of this object characterization activity include several data comparisons that address visibility and photometric data acquired at the detection and recognition distances for all objects under all VES types. It is important to note again that the IR systems cannot be analyzed photometrically because their results are not directly visually based, but instead they are perceived in an electronic imaging system; however, the photometric data can indicate use of the system for object detection.

The results are presented in terms of luminance, background luminance, contrast, and visibility level for the visible conditions followed by an assessment of the IR system usage. Finally, the age analysis is presented.

VISIBLE SYSTEMS SUMMARY OF IR CLEAR RESULTS

Table 6 summarizes the VIS system results from the IR Clear study.

Table 6. VIS systems corresponding to minimum and maximum VIS system distances for detection and recognition.

| Object | Min Detection | Max Detection | Min Recognition | Max Recognition |
|----------------|---------------|---------------|-----------------|-----------------|
| Arrow | HID 2 | HLB | HID 2 | HLB |
| BlackLF | HID 2 | HLB | HID 2 | HLB |
| BlackRT | HID 2 | HLB | HID 2 | HLB |
| BloomLF | HID 2 | HLB | HID 2 | HLB |
| BloomRT | HID 2 | HLB | HID 2 | HLB |
| BlueLF | HID 2 | HLB | HID 2 | HLB |
| BlueRT | HID 2 | HLB | HID 2 | HLB |
| Dog | HID 2 | HLB | HID 2 | HLB |
| FOALT | HID 2 | HLB | HID 2 | HLB |
| FOART | HID 2 | HLB | HID 2 | HLB |
| LFtrnLF | HID 2 | HLB | HID 2 | HLB |
| LFtrnRT | HID 2 | HLB | HID 2 | HLB |
| Rec 30/55 | | | HID 2 | HID 1 |
| Rec Stop/Yield | | | HID 2 | HLB |
| RRPM | HID 2 | HID 1 | HID 2 | HLB |
| RTtrnLF | HID 2 | HLB | HID 2 | HLB |
| RTtrnRT | HID 2 | HID 1 | HID 2 | HID 1 |
| Sign 1 | HID 2 | HLB | HID 2 | HID 1 |
| Sign 2 | HID 2 | HLB | HID 2 | HID 1 |
| Tire | HID 1 | HLB | HID 2 | HLB |

In general, the HLB headlamps provided the longest detection and recognition distances, and the HID 2 headlamps provided the shortest distances of the three VIS systems tested.

PHOTOMETRIC ANALYSIS

The photometric data from the visible-light sources (i.e., HID 1, HID 2, and HLB headlamps) are presented in terms of the pedestrian, retroreflective, and obstacle object types. The first consideration was the comparison of the data for the detection and recognition distances. This was followed by a consideration of each of the data types. It should be noted that in the visibility level analysis, only the modeled results for the older drivers from the IR Clear study were presented because the relationships between each VES performance would be similar regardless of the age of the observer.

Comparison of Detection and Recognition Values

During the IR Clear study, the participants were asked to identify when they first detected the object and then when they recognized it. The photometry of the objects was performed at the mean distance for both of these conditions. During the experiment, several participants reported simultaneous detection and recognition. To investigate this, a comparison of the photometric data for both the detection and recognition characterizations was performed. This allowed for the quantification of the difference between the lighting requirements for detection and recognition.

To identify this difference, a Pearson r-correlation analysis was performed between the data for detection and the data for recognition. This comparison was performed for each of the object types and data types. Table 7 shows the results of this comparison. It can be seen that a relatively high correlation exists between the data values for detection and recognition.

Table 7. Pearson-r correlation results between detection and recognition by data and object type.

| | Pedestrian (N = 66) | Obstacle (N = 21) | Retroreflective (N = 33) |
|-------------------------|--------------------------------|------------------------------|-------------------------------------|
| Luminance | 0.816 | 0.565 | 0.862 |
| Background | 0.677 | 0.817 | 0.646 |
| Contrast | 0.597 | 0.904 | 0.798 |
| Visibility Level | 0.624 | 0.904 | 0.957 |

The comparison of the luminance of the pedestrian objects is shown in figure 34. It can be seen that with a few exceptions, the values for detection and recognition are very similar. A comparison of the standard error shows that in most cases there is no statistical difference between these values.

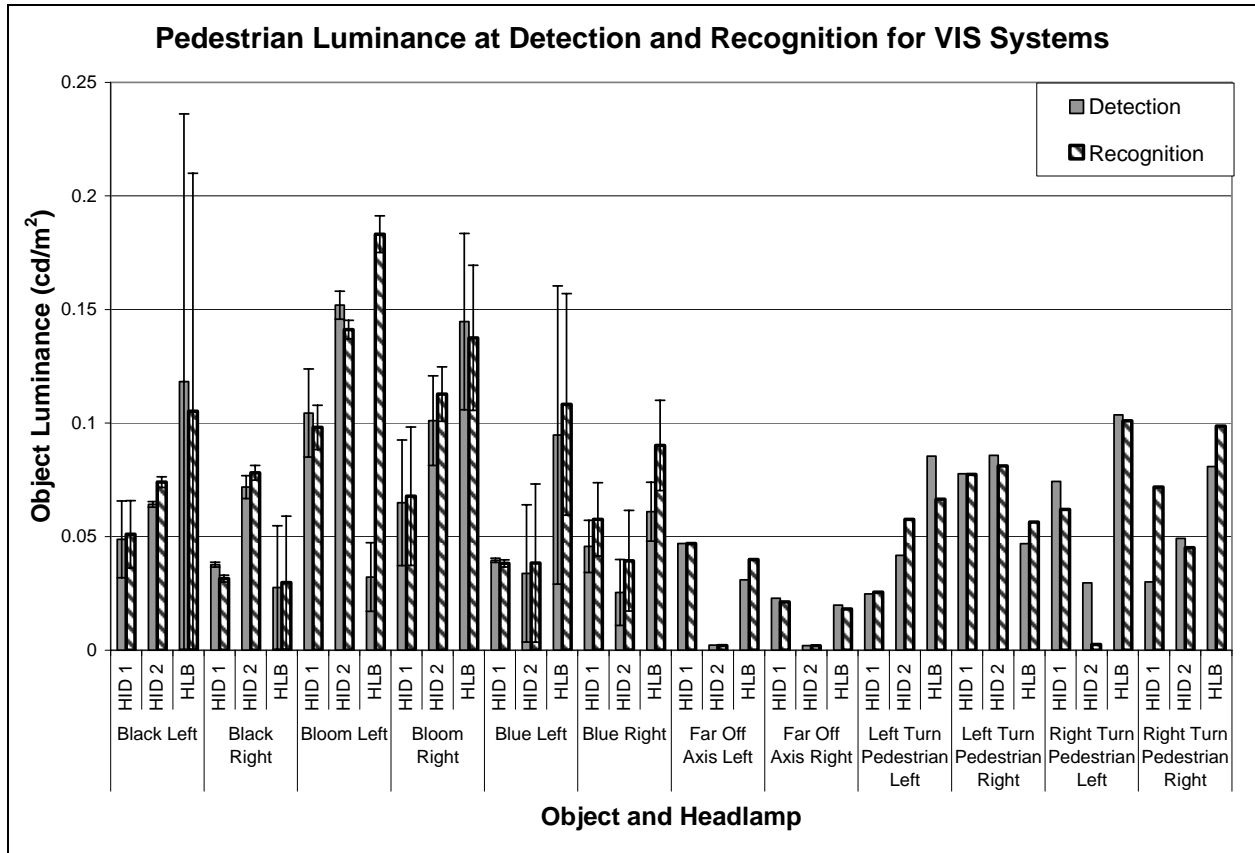


Figure 34. Bar graph. Comparison of object luminance at detection and recognition of pedestrian objects.

Figure 35 shows the luminance comparison for the retroreflective objects, and figure 36 shows the comparison for the obstacle objects. It can be seen that the same trend exists for both of these object types. These results imply that in general, there is no difference between the lighting required for detection and recognition of the objects included in this investigation. Based on this finding, only the detection results will be given further consideration in the photometric analysis.

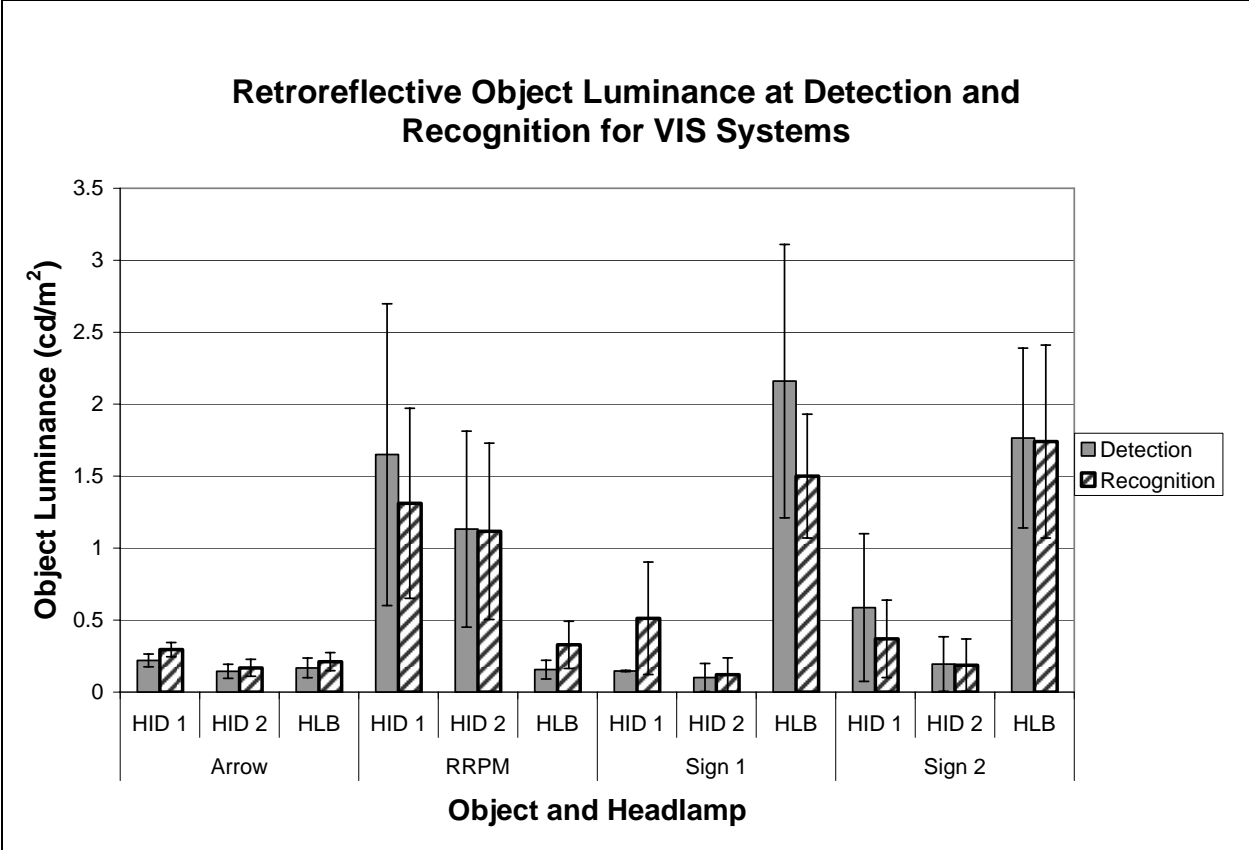


Figure 35. Bar graph. Comparison of object luminance at detection and recognition of retroreflective objects.

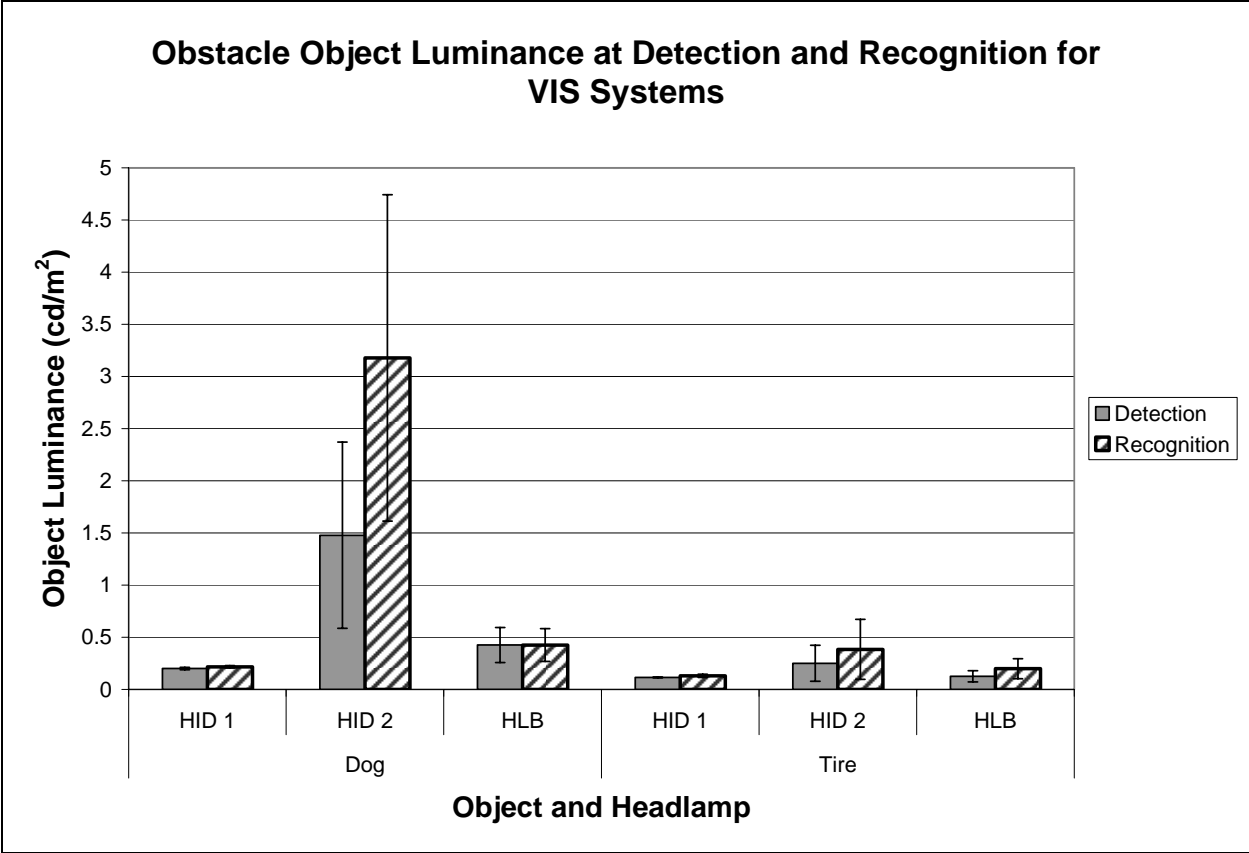


Figure 36. Bar graph. Comparison of object luminance at detection and recognition of obstacle objects.

Pedestrian Object Group

The analysis of the pedestrian object group included the 3 VIS headlamps and all 12 pedestrian object scenarios. These involved pedestrians standing at different locations, facing the vehicle, and wearing black or denim clothing. The means of their luminance, background luminance, contrast, and visibility level results are presented with standard error bars. The exceptions are the objects appearing far off axis and objects in curves; these appeared at only one location, so no standard error value is available.

VIS Headlamp and Pedestrian Object Effect on Luminance

The effect of the pedestrian object types on the object luminance at detection for VIS headlamps is shown in figure 37. In this figure, it can be seen that the two bloom objects both required the highest luminance for detection. It would be expected that higher luminance is required to

overcome the disability glare of the headlamps. The Bloom Left object had a higher luminance at detection than the Bloom Right object, indicating that closer proximity to the glare source results in a higher level of disability glare.

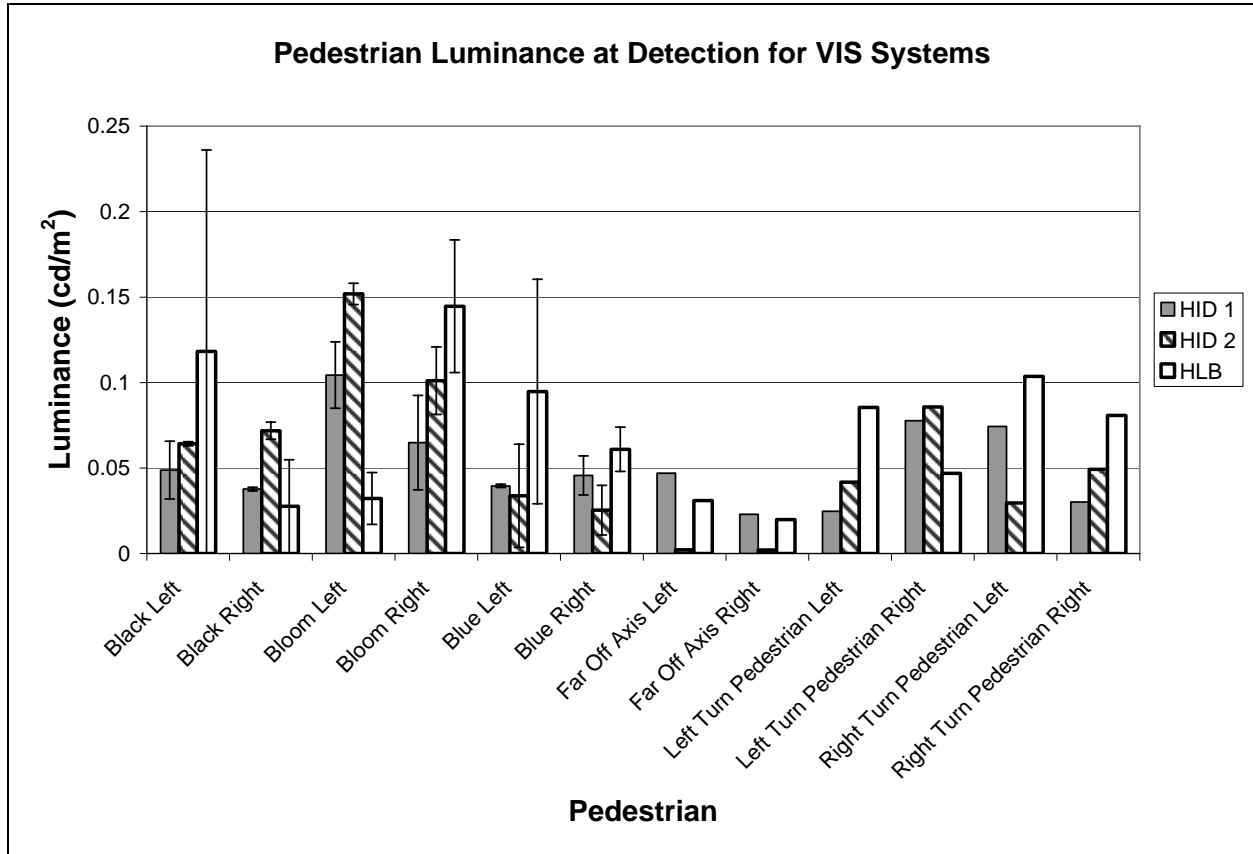


Figure 37. Bar graph. Mean luminance values at pedestrian object detection.

The other interesting aspect of this comparison is that in general, the HID 1 system required lower luminance for detection than the HID 2 system, which has a generally lower luminance than the HLB system. This was the case for all objects except those that were far off axis or on the left. In these cases, the luminance provided by the HID 2 system was very low. These headlamps have a wider beam distribution, leading to the expectation that the luminance provided to the side would be higher than the other configurations.

One of the issues with this comparison is that all of these measurements were taken at the mean detection distance. One would expect that, with the exception of the bloom condition, a similar luminance would be required for detection of any of the pedestrian objects. As the vehicle approached, detection would occur when the required luminance was achieved; however, the

pedestrian objects did not have a consistent threshold luminance value. This is particularly noticeable when comparing the threshold luminance value for a given object when it is on the left versus on the right. Regardless of lateral position, the object should have a similar size and, therefore, a similar required luminance. This means that object luminance is a poor indicator of object visibility. Other factors, such as the background or displacement from the driver's line of sight, may come into play in this detection and recognition task.

VIS Headlamp and Pedestrian Object Effect on Background Luminance

The effect of the headlamp type on the background luminance for the various experimental objects is shown in figure 38, where it can be seen that the background provided by each of the headlamps is similar for most objects. Significant differences can be seen only in the far off-axis conditions, where the HID 2 system provided a very low background luminance. It should be noted that although this system had the widest beam pattern, it also had the lowest detection distance (27.1 m or 89 ft), meaning that the angular eccentricity of the object likely put it outside the beam of the headlamps.

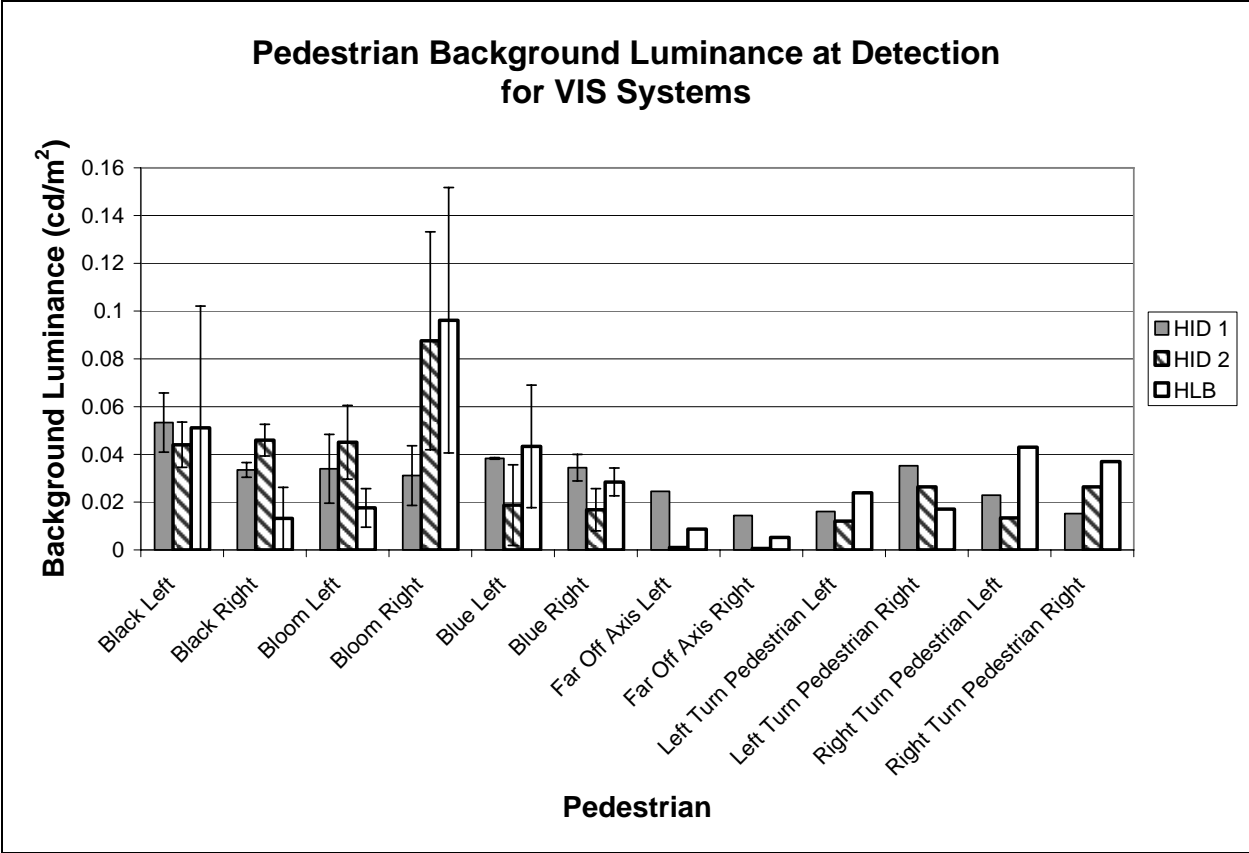


Figure 38. Bar graph. Mean background luminance values at pedestrian object detection.

In this relationship, the Bloom Right was observed with a relatively high mean background luminance level as compared to the other objects. When measuring background luminance in these instances, the bloom vehicle headlamps were not turned on and the pedestrian was on the opposite side of the road from the vehicle. In this instance, objects behind the pedestrian such as guardrails and roadway infrastructure would increase the background luminance. Because a high standard error is associated with the measurement, it can be expected that the various locations where the object appeared would contribute to this high background luminance value.

VIS Headlamp and Pedestrian Object Effect on Contrast

For the headlamp and pedestrian type relationship, the contrast was measured at the point of detection, which implies that this was the actual threshold contrast for the object. It would be expected that the threshold would be similar for all of the pedestrian objects presented because the size of the objects was similar. The exceptions to this expectation are the bloom scenarios, where a higher contrast was needed to overcome the glare, and in the off-axis and curve

scenarios, where the object was eccentric to the line of sight. The effect of the visible headlamp type and the pedestrian type on the contrast is shown in figure 39. The figure shows the higher contrast for the off-axis and the bloom scenarios, as expected. The item to notice is that in the Black Left, Black Right, Blue Left, and Blue Right object conditions, the HLB headlamps had the highest threshold contrast. For the black-clothed objects, the HID 1 system had the lowest threshold contrast, with the black-clothed left pedestrian having a negative contrast level.

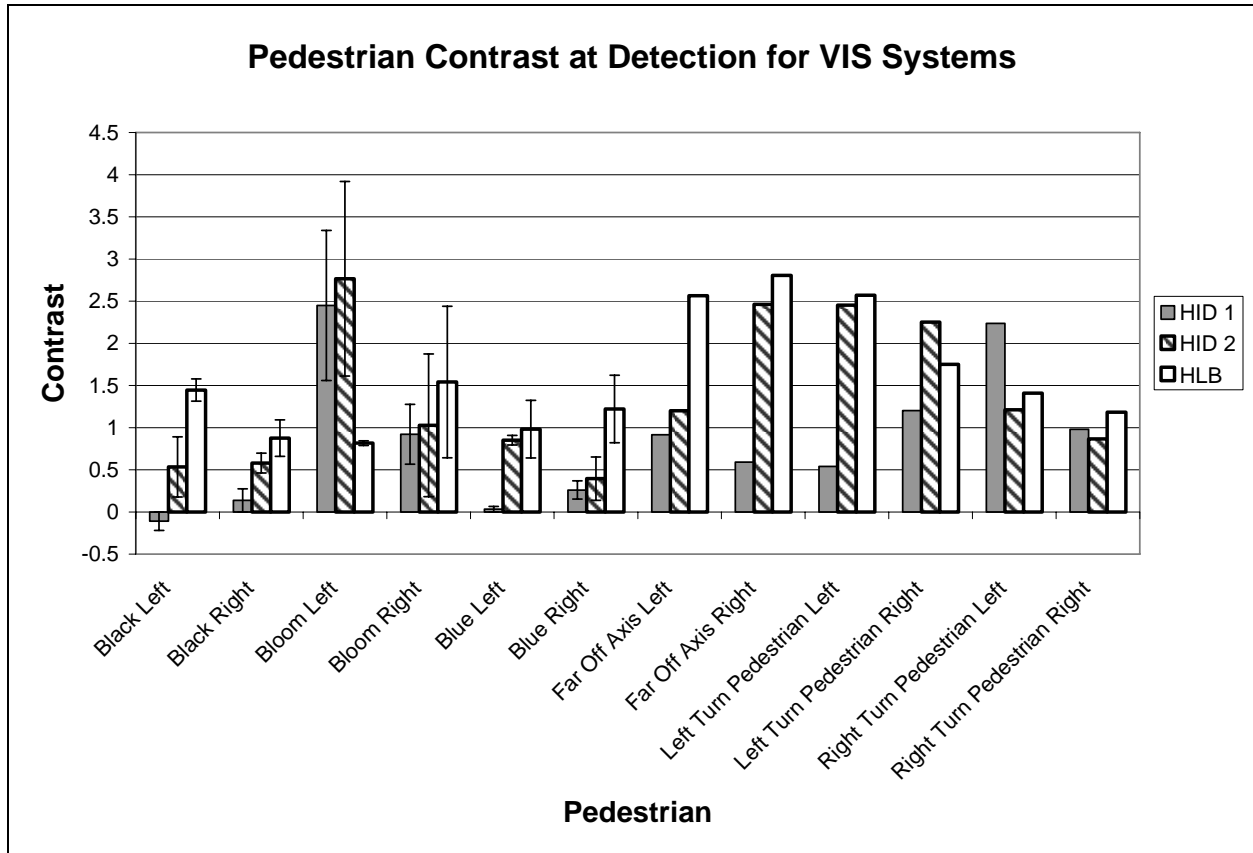


Figure 39. Bar graph. Mean contrast values at pedestrian object detection.

It is also noteworthy that the contrast for the off-axis objects for the HID 2 system was similar to that of the HLB system. This indicates that as the vehicle approached the object, the required threshold contrast was not met until the very short distance found in the IR Clear study.

VIS Headlamp and Pedestrian Object Effect on Visibility Level

As with the contrast calculation, the threshold visibility level should be similar across all of the pedestrian objects and VIS system types. Again, a slight increase in threshold visibility level for

the bloom, off-axis, and curve pedestrian objects would be expected. The results of this calculation for all of the pedestrian and visible headlamp types are shown in figure 40.

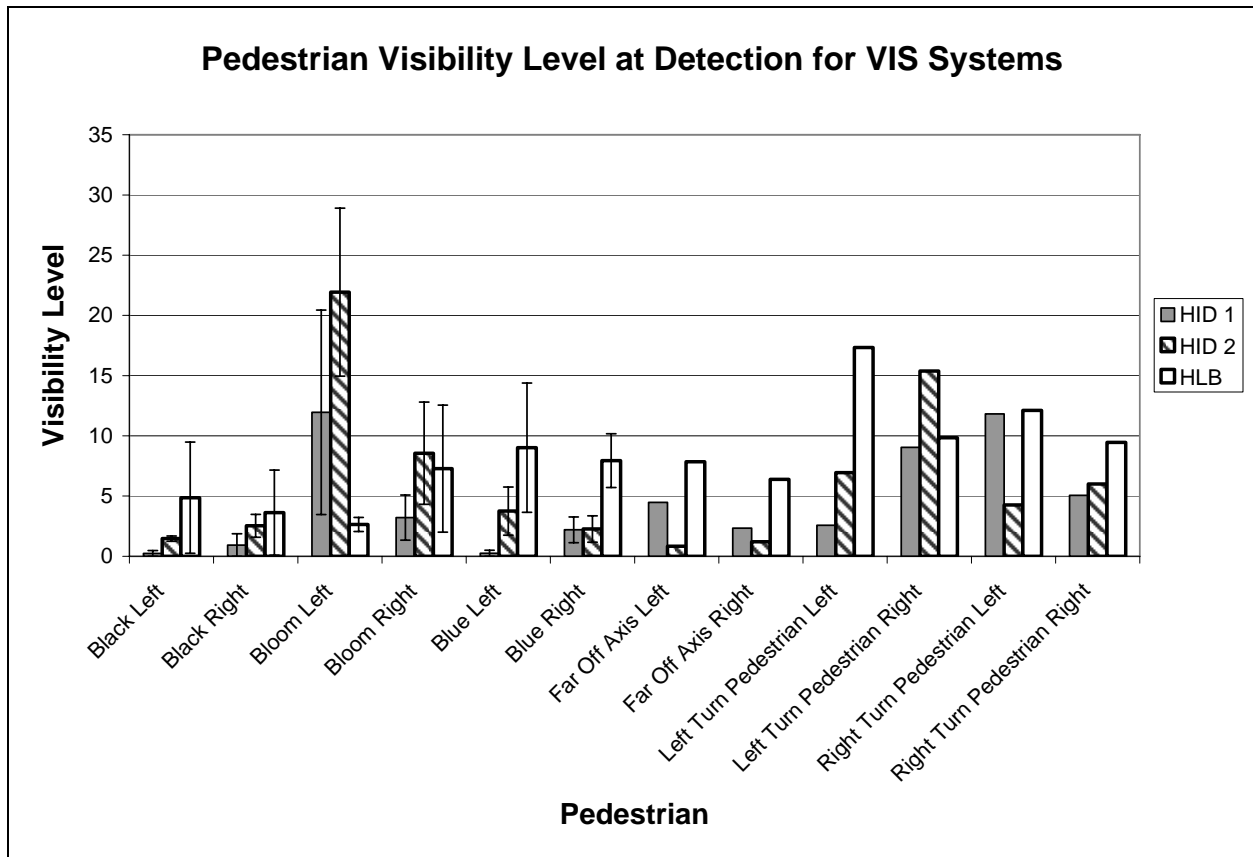


Figure 40. Bar graph. Older driver mean visibility levels at pedestrian object detection.

The consistency of the values seen in the contrast calculation is not evident in the visibility level calculation. The increase for the bloom and the off-axis conditions is seen, but the black-clothed pedestrian and the blue-clothed pedestrian had different visibility level values. For the blue-clothed objects, the HLB system provided a higher visibility level at threshold than did the HID 1 and HID 2 systems. In general, many of the objects had a high standard error associated with the measurement, so many large differences existed, but they were not statistically significant.

One of the reasons for the dissimilarity in visibility level across the types of headlamps might be the object size. The visibility level accounts for the object size and the vehicle headlamp cutoff. Both of the HID systems had a cutoff-style headlamp that cut the beam pattern in a sharp line, permitting very little light above it. The HLB system did not have this cutoff, and because of an

anomaly in the aiming method used, there was significant light aimed straight down the roadway. This means that a tall object would have been more consistently illuminated by the HLB headlamps than by the cutoff HID headlamps. As a vehicle with cutoff headlamps approached an object in the roadway, the lower part of the object would have been illuminated first, and then the lighted area would have moved up the body as the headlamps approached, making more of the object visible below the cutoff line. For example, figure 41 shows the pedestrian in a right turn, right side in the HID 2 condition, and figure 42 shows the pedestrian in a right turn, right side in the HLB condition. The unevenness of the luminance in the HID 2 condition shows the influence of the cutoff line. (Note that the photometric detector captured these images at long distances, so some granularization of the images has occurred.)

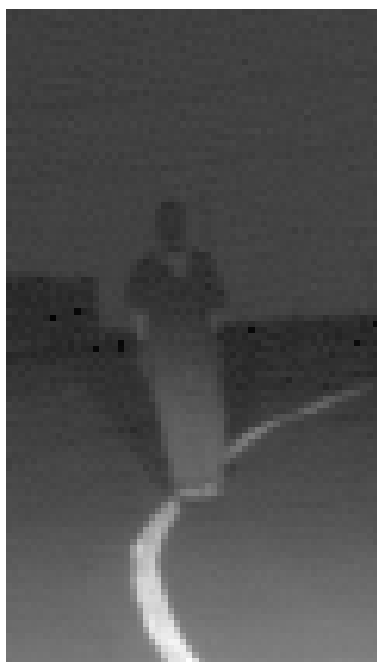


Figure 41. Picture. Right turn right pedestrian in HID 2 condition.



Figure 42. Picture. Right turn right pedestrian in HLB condition.

In the visibility level calculation, the entire object size was used, and it was assumed that the object was evenly illuminated; however, the case just described might lead to discrepancies in the evaluation of the visibility level of the object.

VIS Headlamp and Obstacle Object Group Analysis

The next set of results is from the analysis of the obstacle object group, which consists of the tire tread and the simulated dog. They represent roadway objects typically smaller in size than a pedestrian. Like the pedestrians, the analysis of this object group is based on the comparison of the means of the luminance, background luminance, contrast, and visibility level.

VIS Headlamp and Obstacle Object Effect on Luminance

Figure 43 shows the luminance of the two obstacle objects at the threshold distance. In both cases, the HID 2 headlamps provided a higher luminance at threshold than either the HLB or the HID 1 headlamps. The dog was located on the centerline of the road, and the tire tread was placed on the edgeline. Because the HID 2 system had the widest beam pattern, it is likely that these objects were illuminated at a higher level by the HID 2 system than by the other lighting systems. It also must be remembered that the HID 2 system produced the shortest detection distances for the three visual VESs.

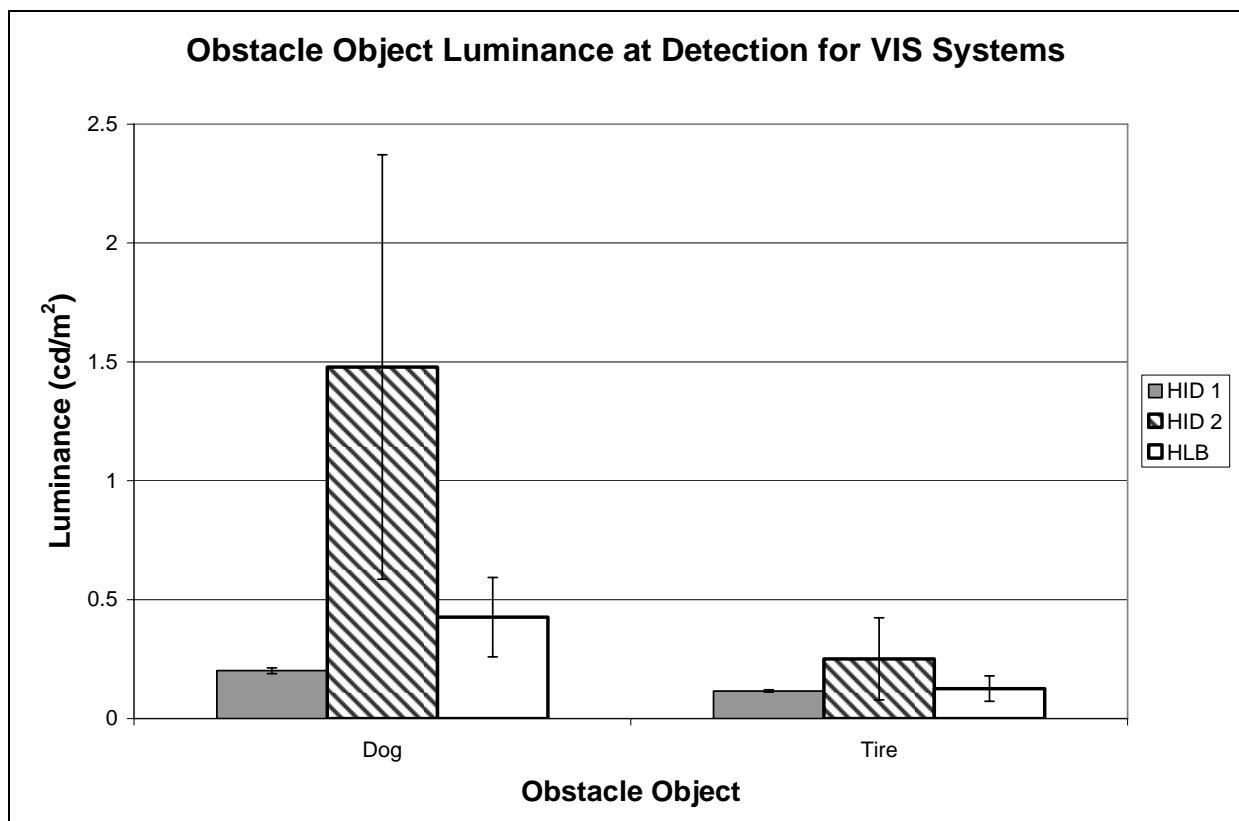


Figure 43. Bar graph. Mean luminance values at obstacle object detection.

As with the pedestrian objects, the luminance does not provide a consistent threshold value. This means that the luminance is not a reliable measure of visibility.

VIS Headlamp and Obstacle Object Effect on Background Luminance

Figure 44 presents the effects of VIS headlamp and obstacle object for the background luminance levels of each obstacle object. Because both of these objects were low and close to the road surface, the measured luminance was primarily the luminance of the pavement.

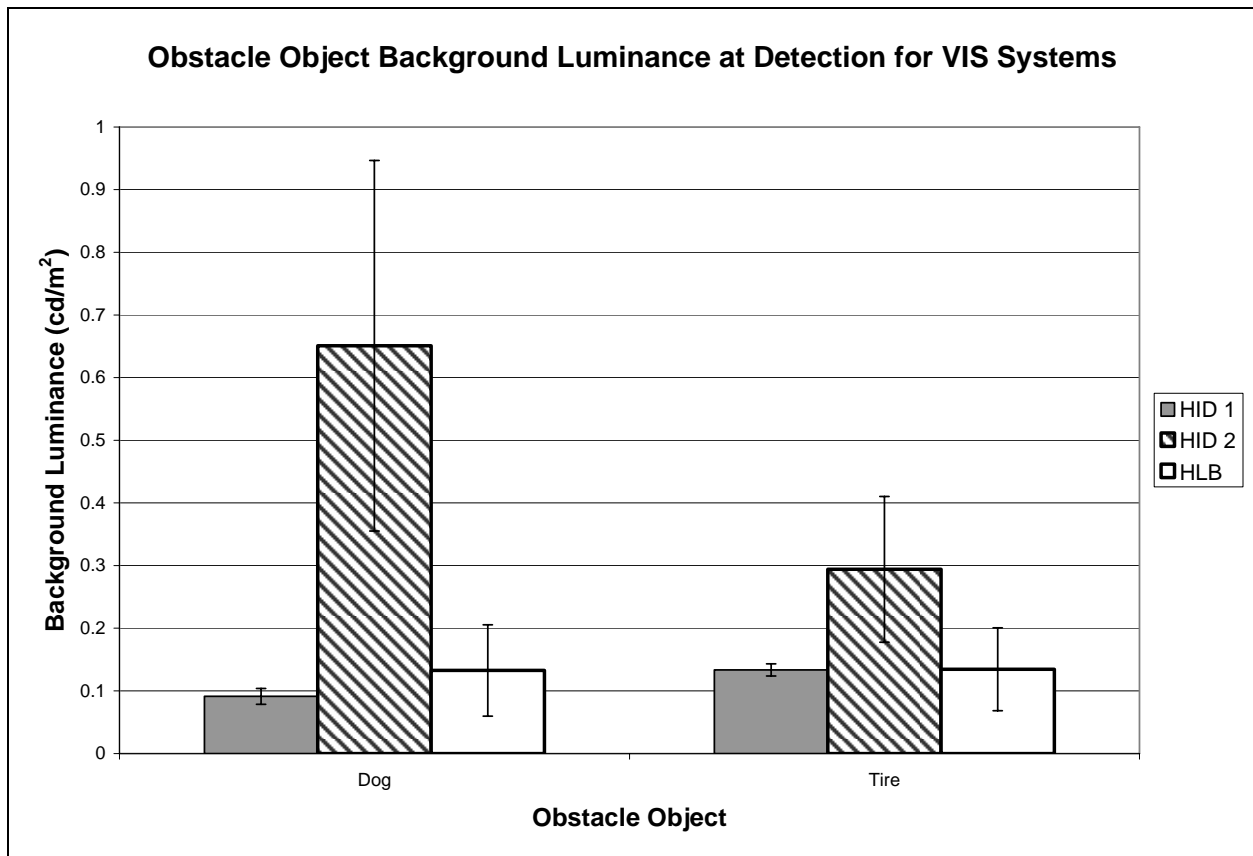


Figure 44. Bar graph. Mean background luminance values at obstacle object detection.

As in the object luminance comparison, the HID 2 headlamps had the highest background luminance, followed by the HLB and HID 1 headlamps. There was no significant difference between the HID 1 and HLB systems, but the HID 2 system was significantly different. Again, this was likely a result of the HID 2 system producing the shortest detection and recognition distances.

VIS Headlamp and Obstacle Object Effect on Contrast

The contrast relationship for the obstacle objects are presented in figure 45. It is noteworthy that the tire tread, which was black with a very low reflectance, had negative contrast, which means that the object is darker than the background. The dog was gray and was brighter than the pavement surrounding it. From the analysis of the standard error, no significant difference exists between the HID 1 and HID 2 systems for either the dog or the tire tread. The HLB system does show a significant difference from the other two headlamp systems.

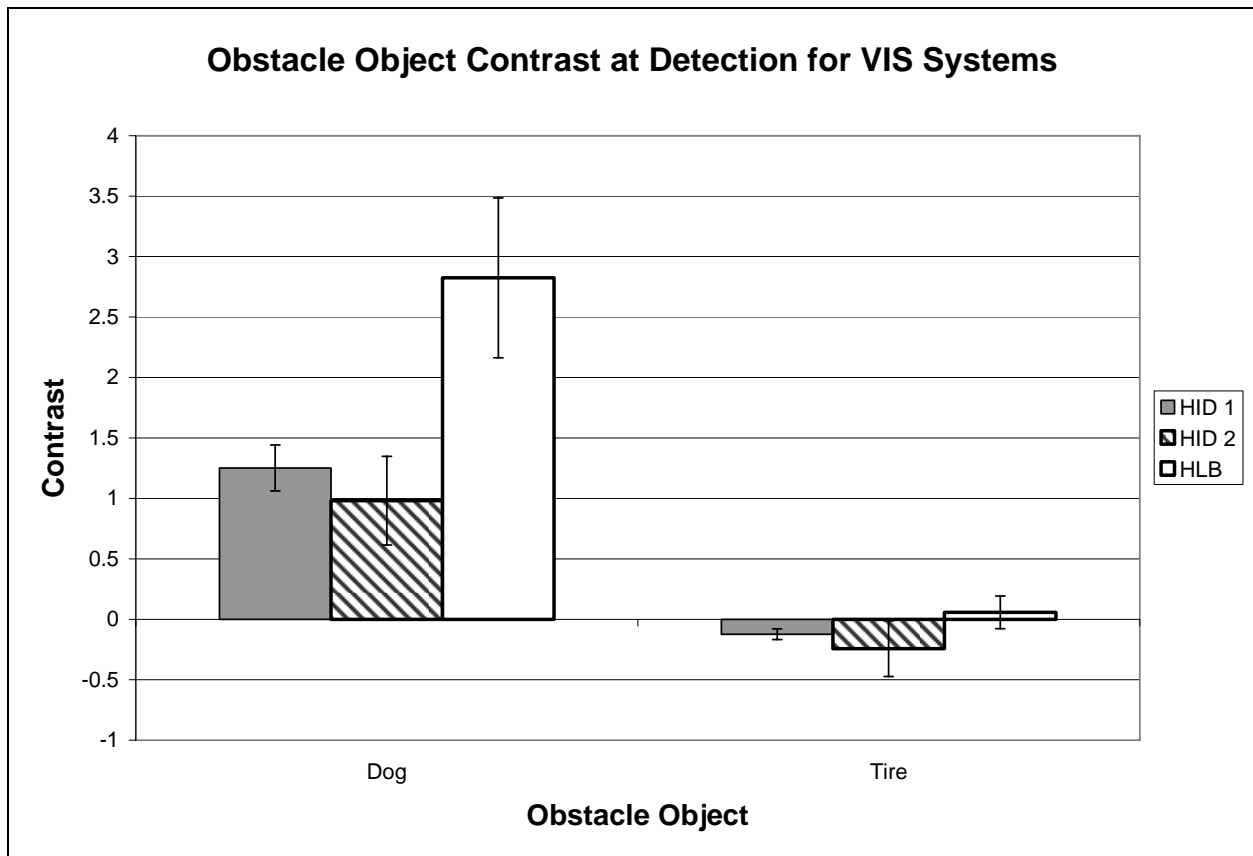


Figure 45. Bar graph. Mean contrast values at obstacle object detection.

Table 6 also shows that the HLB system was associated with the maximum detection and recognition distances of the VIS systems for both the dog and tire objects. The HLB system's superior performance over the other systems is also indicated by its higher contrast at threshold.

VIS Headlamp and Obstacle Object Effect on Visibility Level

The effects of VIS headlamp and obstacle object on visibility level are shown in figure 46. In this calculation, as with the pedestrian objects, a similar threshold visibility level value would be expected for all of the objects and VESs, and indeed, there was no significant difference between the HID 1 and HID 2 systems for the simulated dog object. On the other hand, the HLB system produced the highest threshold visibility level. For the tire tread object, there was no significant difference between the HID 1 and the HLB system, with the HID 2 system having a higher threshold visibility level than the others, although it was not significantly different from the HLB system.

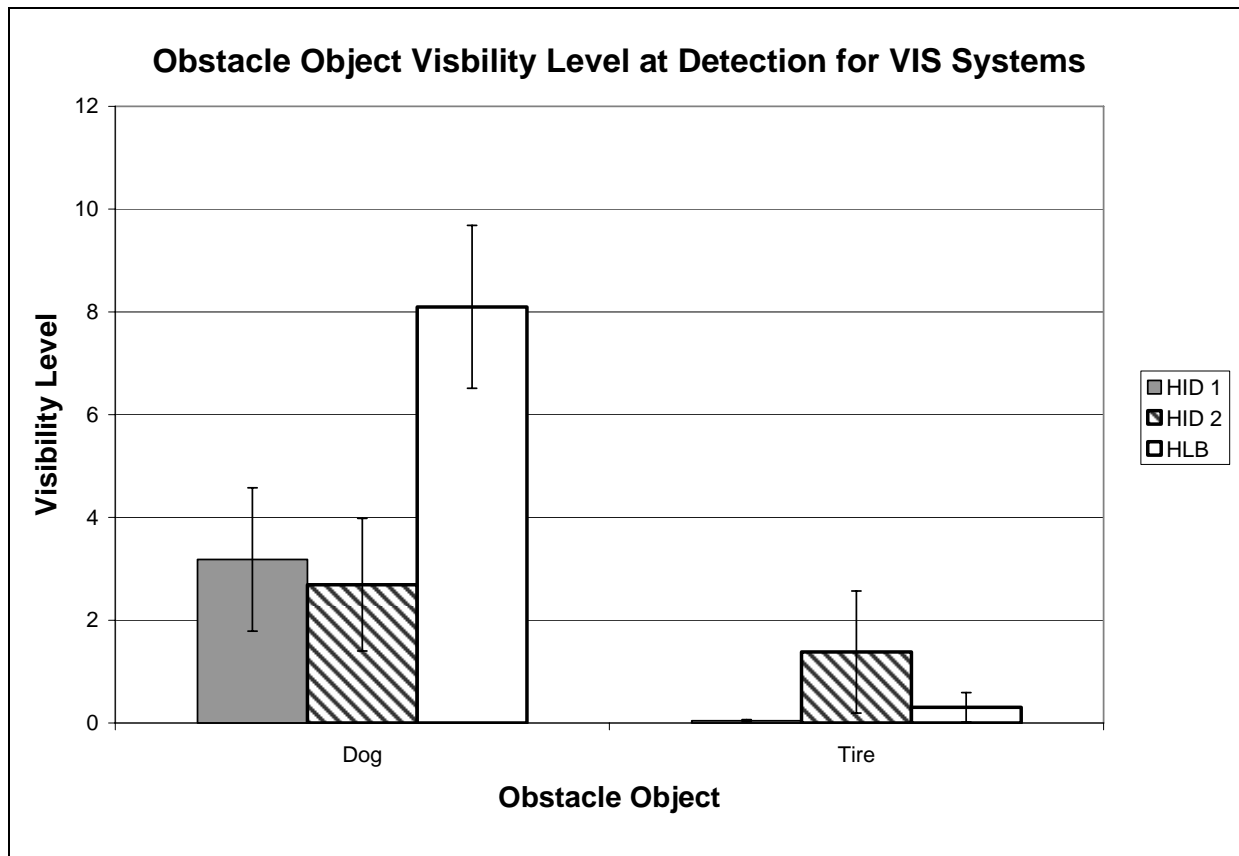


Figure 46. Bar graph. Older driver mean visibility levels at obstacle object detection.

The dog's highest visibility level was produced by the HLB headlamps, which suggests that the HLB headlamps allowed earlier detection of the dog compared to the other headlamps tested. At the shortest detection distance, the HID 2 headlamps did not produce a large difference in visibility levels.

The difference between the performance of the HID 2 system for the dog and for the tire likely resulted from the beam pattern. The HID 2 system has the widest beam pattern, and it will light an object on the right-hand side of the road more effectively than one in the center of the road. The opposite occurs for the HLB system, which produced a higher visibility level with the dog than with the tire tread. This is likely because the aim of the HLB headlamps is pointed more toward the center of the road than to the right edge.

The similar visibility level of the HID 1 and HID 2 system for the dog is expected, and this represents the threshold value for these objects, which do not have the size issues that are evident with the pedestrian objects.

VIS Headlamp and Retroreflective Object Group Analysis

This analysis examined the retroreflective objects, which are designed to reflect light back to the light source rather than reflect diffusely, as the pedestrians and the obstacle objects do. The retroreflective objects included the turn arrow, the raised retroreflective pavement marker, and the two sign configurations. The IR Clear study included two additional recognition tasks: differentiating between 30- or 55-mi/h speed limit signs, which required participants to read the speed limit, and recognizing the difference between a stop and a yield sign. The object characterization results for all the retroreflective objects were analyzed for both detection and recognition.

It should be noted that because of the long distances at which these were seen, the resulting visual size was very small, and these measurements have a high uncertainty associated with them because it is extremely difficult to measure a small light source with a CCD camera.

VIS Headlamp and Retroreflective Object Effect on Luminance

The objects in the retroreflective group had much longer detection distances than did the other objects. It should be noted that these distances are so long that they normally would be considered outside of the reach of the vehicle headlamps. Figure 47 shows the results of these measurements. No significant difference resulted between headlamp types for the turn arrow, which lay flat on the road surface; each headlamp performed equally well in this situation. No significant difference resulted between the two HID systems for the RRPM, which also lay on

the roadway, but the HLB system provided a much lower luminance. Conversely, the results for the two sign detection tasks showed the HLB system provided a much higher luminance than the HID systems.

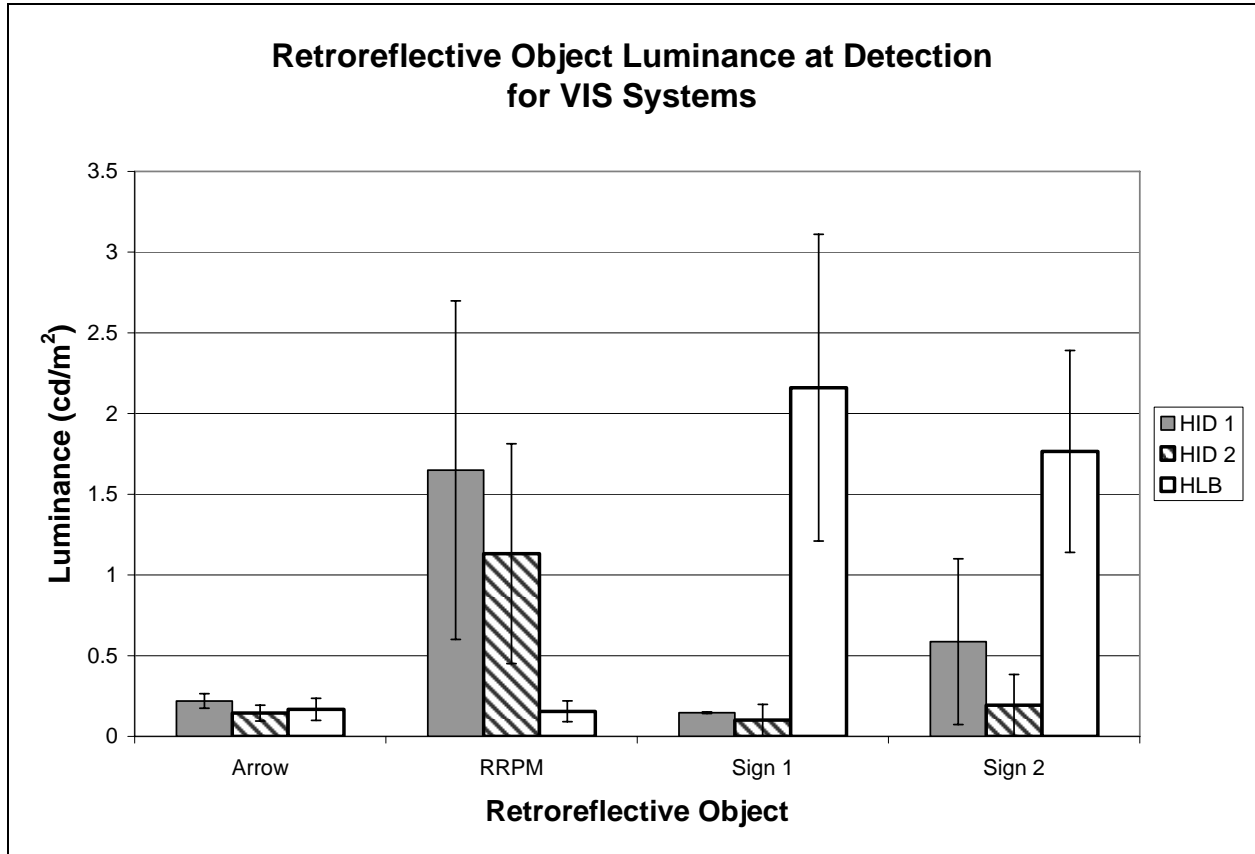


Figure 47. Bar graph. Mean luminance values at retroreflective object detection.

The geometry and aiming of the headlamps is critical for this measurement. Because the HID headlamp beam profiles had a cutoff and the HLB headlamp beam profiles did not, the HLB headlamps provided a higher illuminance on the signs, resulting in a higher luminance level than did the HID headlamps; however, it is not clear why the RRPMS were lit to a higher level by the HID systems than by the HLB system. This may be a result of the beam distribution of the HID headlamps lighting the roadway centerline area more effectively than the HLB headlamps; these VES types may have equivalent performance in the center of the driving lane directly in front of the driver.

The results for the recognition task are shown in figure 48. In this instance, the luminance of the 30- or 55-mi/h speed limit signs at the recognition distance is significantly higher than that of the

other objects at recognition. The speed limit sign scenario also had the shortest recognition distance, approximately 122.2 m (401 ft) compared to 277.2 m (854.7 ft) for the stop and yield sign recognition task. For this task, the participant had to read the black numbers on the road sign and could not rely on recognizing the sign by shape alone. Thus the legibility distance for the speed limit sign was shorter than the recognition distance for stop and yield signs, and therefore, a higher luminance was measured. The HID 2 system did not perform as well as the other systems in the sign scenarios. According to table 6, the HID 2 VES yielded the shortest recognition distance. This implies that the HID 2 system did not provide the same level of illuminance on the signs as did the other two VESs.

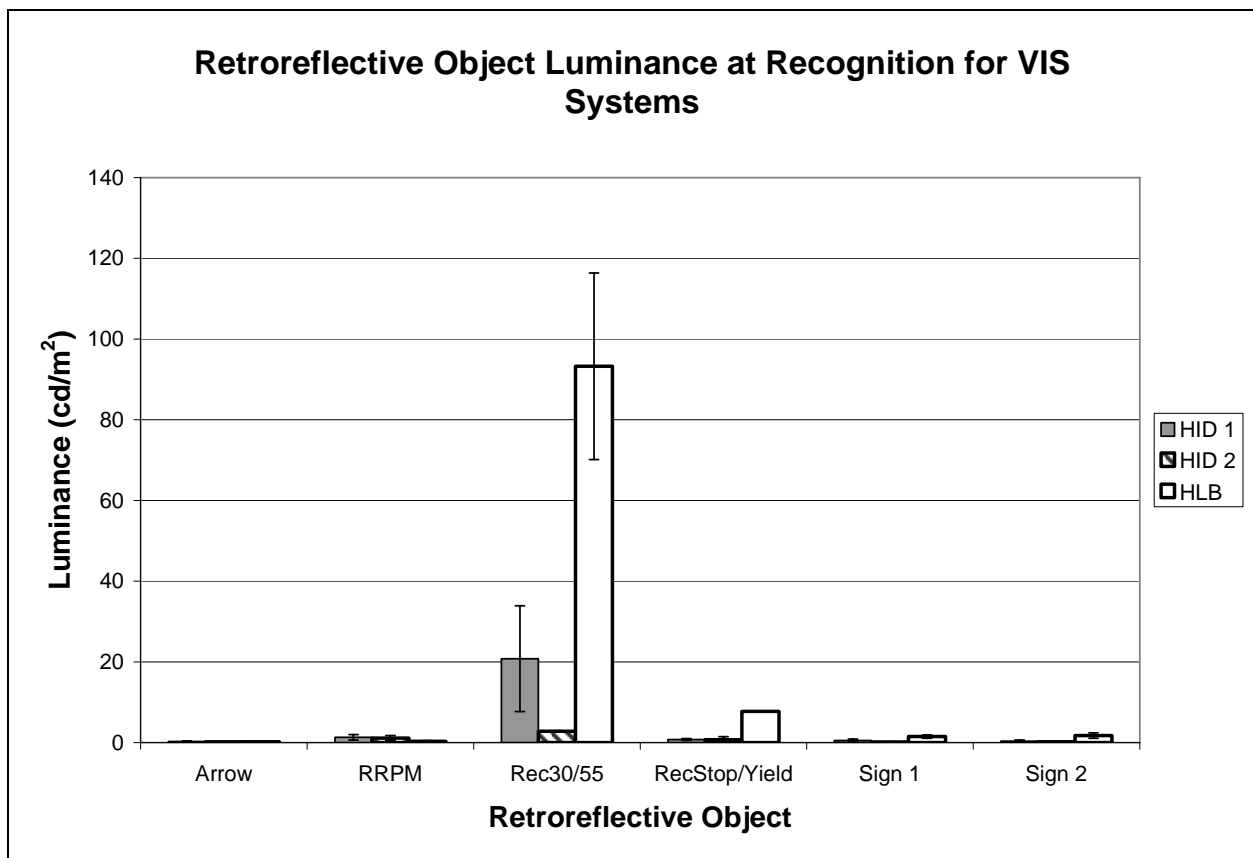


Figure 48. Bar graph. Mean luminance values at retroreflective object recognition.

VIS Headlamp and Retroreflective Object Effect on Background Luminance

The results of the background luminance measurements at detection of the retroreflective objects are shown in figure 49. The backgrounds for these objects were different. For the turn arrow and

the RRPM, the background was pavement; for the signs, the background was landscape and foliage.

In this measurement set, the HID systems did not produce significantly different background luminances for the RRPM and the sign scenarios. The HID 1 system did provide a higher pavement luminance than the HID 2 system for the turn arrow. The HLB system, performed similarly to the HID systems for the turn arrow and the RRPM. The illuminance from the non-cutoff, high-aimed HLB system produced a higher background luminance for the signs than either of the HID systems because of the cutoff associated with the HID beam patterns. A high standard error was associated with the sign background measurements, which indicates the high variability of the background based on sign position.

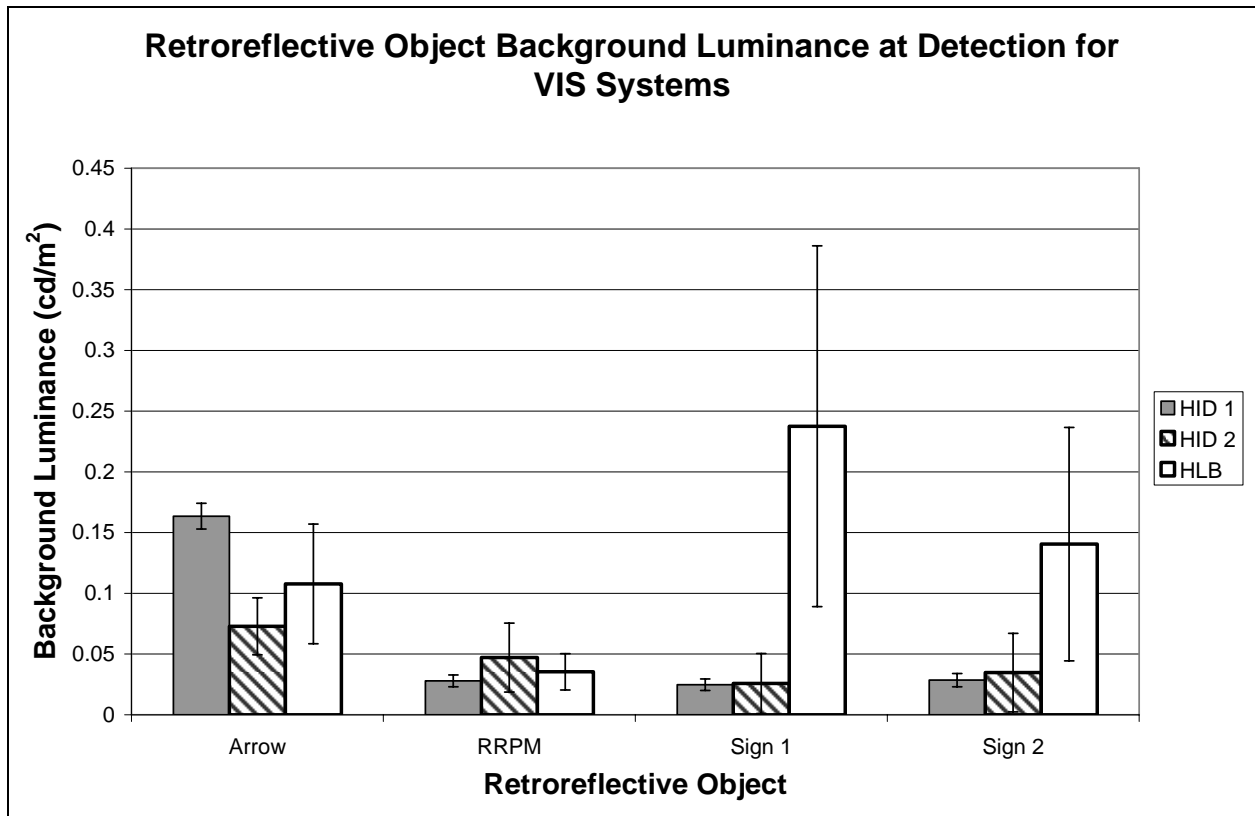


Figure 49. Bar graph. Mean background luminance values at retroreflective object detection.

The background luminance measurements for the retroreflective object recognition task are shown in figure 50. Of interest in this figure are the measurements for recognition of the 30- and 55-mi/h signs and the recognition of the stop and yield signs. For both of these conditions, the

distance to the object was much shorter than that of the detection tasks. The same trend as in the detection task is apparent on the signs: the HID systems had similar performance, and the HLB system provided a higher luminance level. The cutoff of the HID headlamps reduced the background luminance. There was also a high standard error associated with these measurements, demonstrating the importance of the object position.

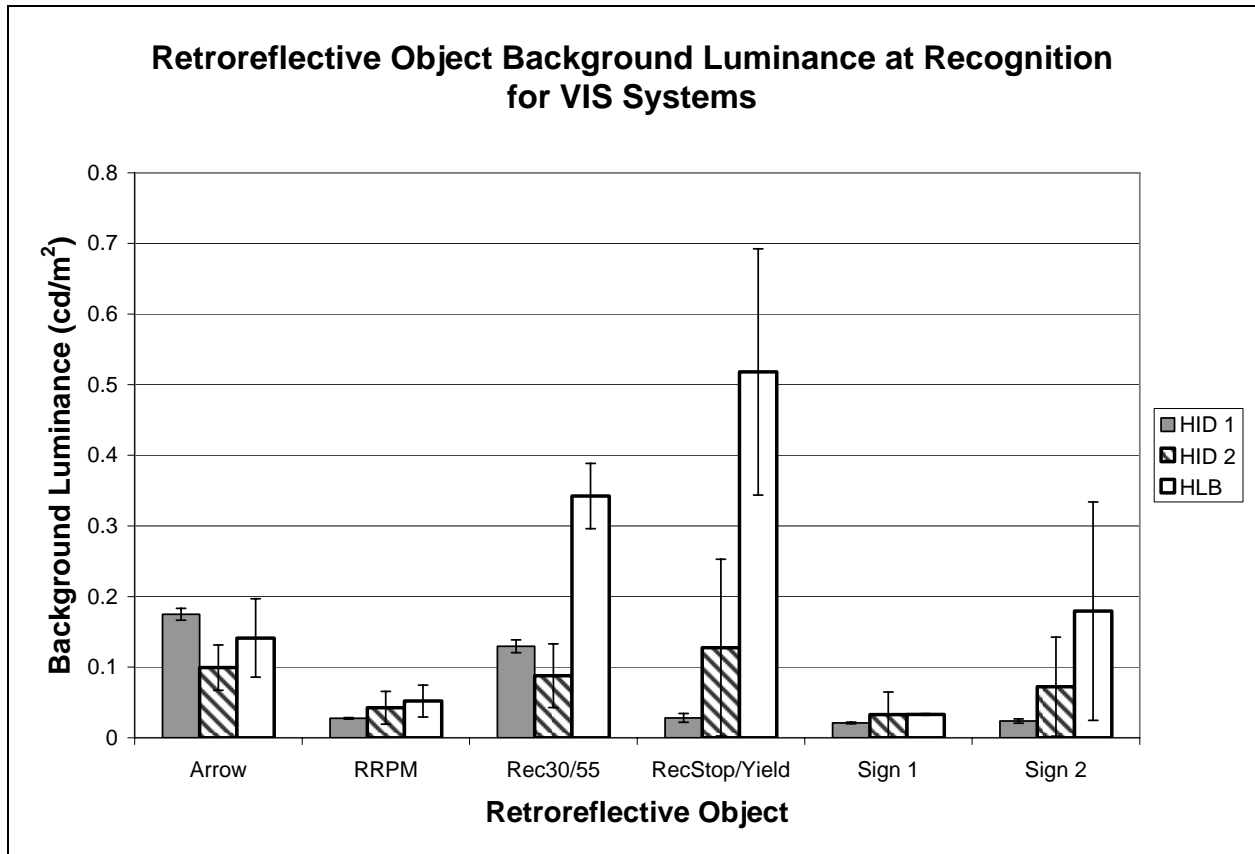


Figure 50. Bar graph. Mean background luminance values at retroreflective object recognition.

VES Headlamp and Retroreflective Object Effect on Contrast

The contrast calculations were performed for all of the retroreflective objects. These results are shown in figure 51. For the turn arrow, the threshold contrast was very low as compared to the other retroreflective objects. This resulted from the low object luminance and the higher background luminance. Similarly for the RRPM, the low background luminance and higher object luminance led to a higher contrast. In this case, the HID 1 system had the highest threshold contrast, followed by the HID 2 and HLB systems. This result might indicate that the HID systems were more effective at lighting the object and did not light the pavement as well, thus allowing the RRPM to have a higher contrast than the other objects. Finally, the HLB system provided the highest contrast for the signs, but it was not significantly different than the HID 1 system. The HID 2 system continued to provide the lowest contrast of all three of the sources. Again, this is indicative of the aiming and cutoff differences between the headlamp beam patterns.

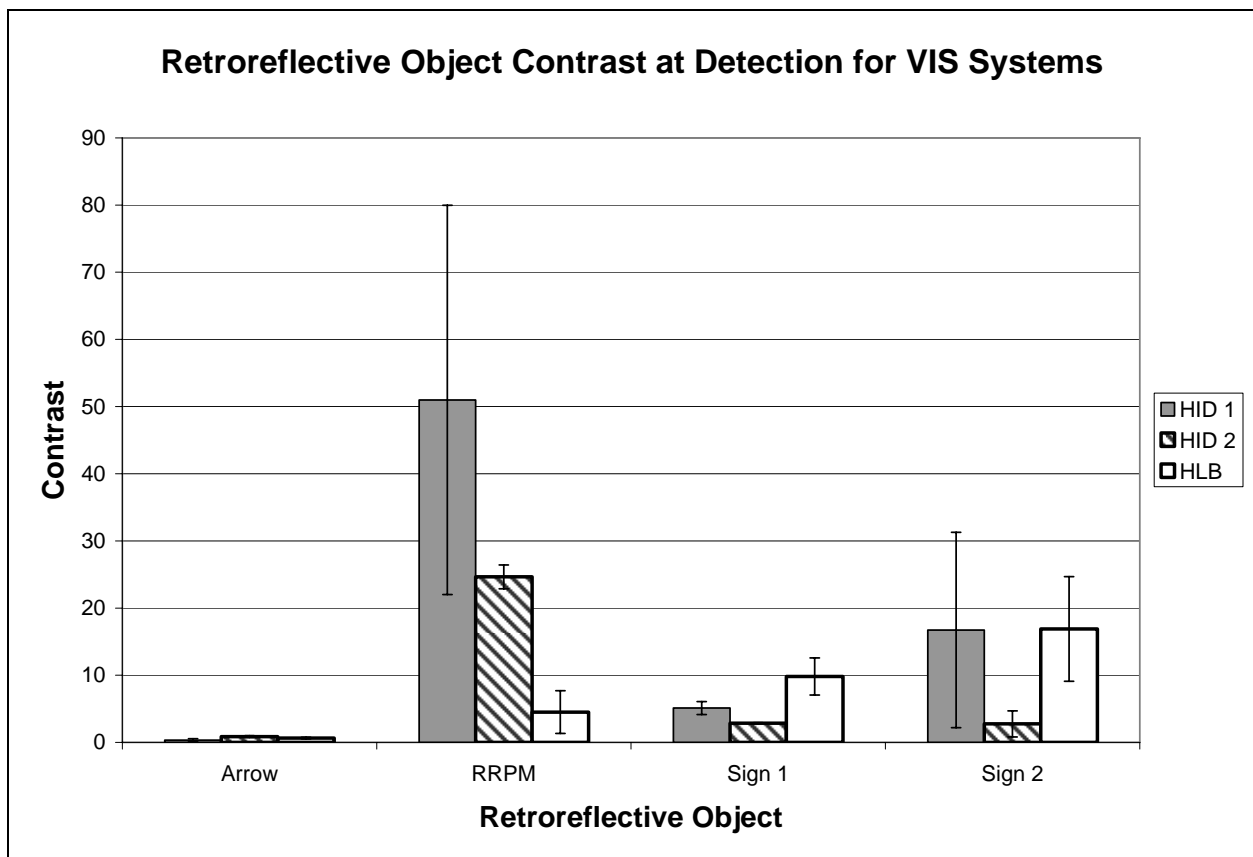


Figure 51. Bar graph. Mean contrast values at retroreflective object detection.

Figure 52 shows the recognition task results for the retroreflective objects. Here again, the 30- and 55-mi/h speed limit sign recognition required the highest threshold contrast, and again the HID 2 system provided the lowest contrast with the shortest recognition distance. This trend is apparent with all of the objects. The recognition task of differentiating between the stop and yield signs produced contrast values similar to that of the initial sign recognition task.

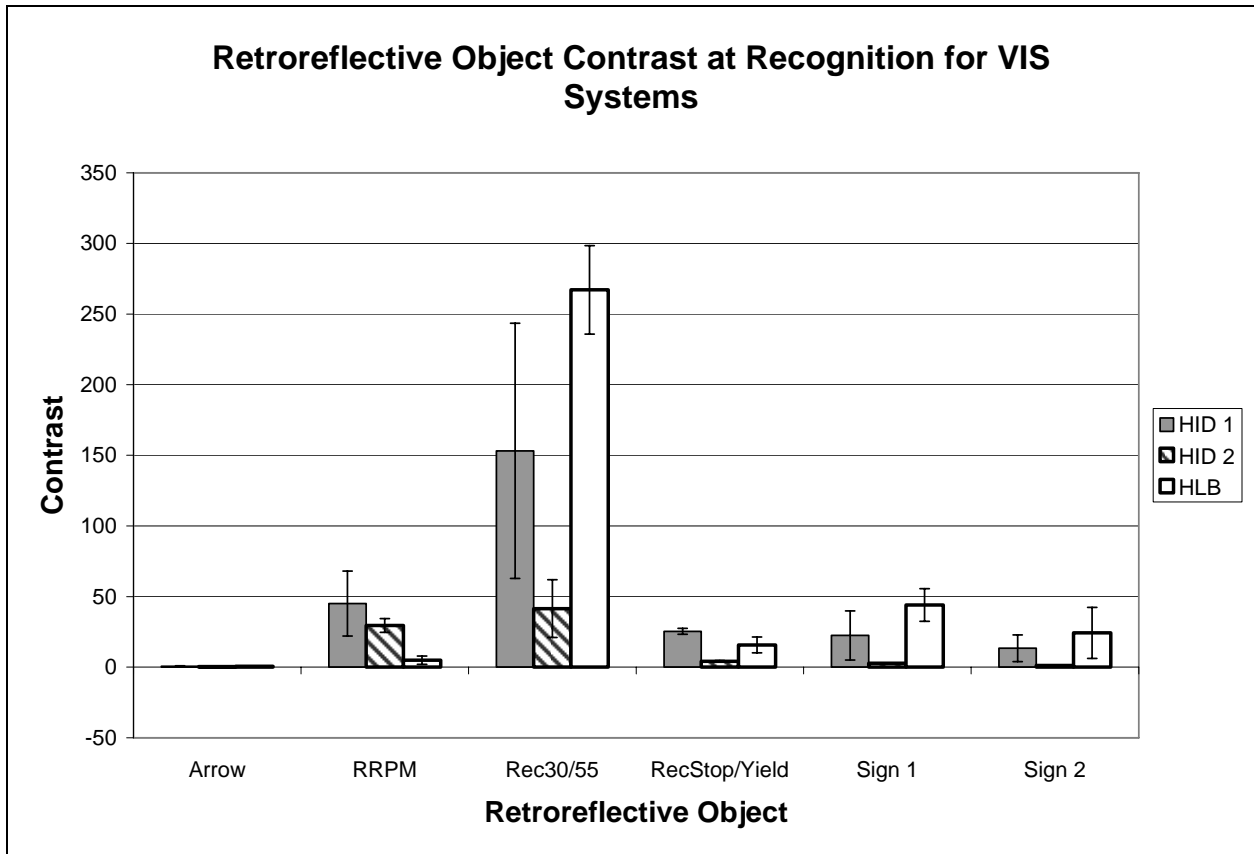


Figure 52. Bar graph. Mean contrast values at retroreflective object recognition.

VIS Headlamp and Retroreflective Object Effect on Visibility Level

As with the other object types, the visibility level would be expected to have a consistent threshold for all of the objects. As seen in figure 53, the results for the turn arrow and RRPM had a very similar visibility level for all headlamp types as compared to the results for the signs. For the signs, the HLB system provided the highest visibility level, which was significantly different than the results for the HID systems. Again, this probably resulted from the cutoff and aim of the HLB system. As with the other variables, the HID 2 system continued to provide the lowest visibility level of all of the tested systems.

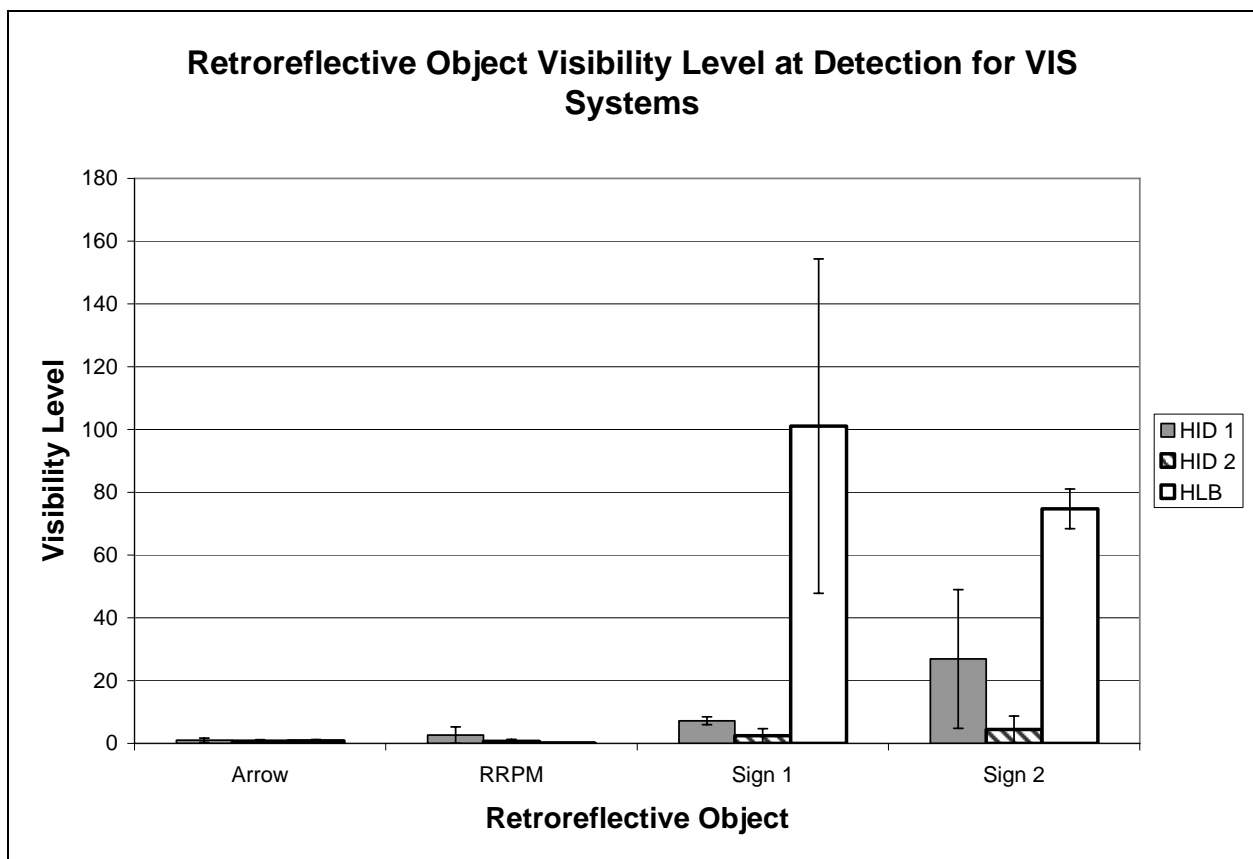


Figure 53. Bar graph. Older driver mean visibility levels at retroreflective object detection.

Figure 54 shows the visibility level for the recognition task. The 30- and 55-mi/h speed limit sign recognition task by far dominates this comparison. The same trend is evident: the HLB system provided the highest visibility level followed by the HID 1 system, and the HID 2 system provided the lowest visibility level.

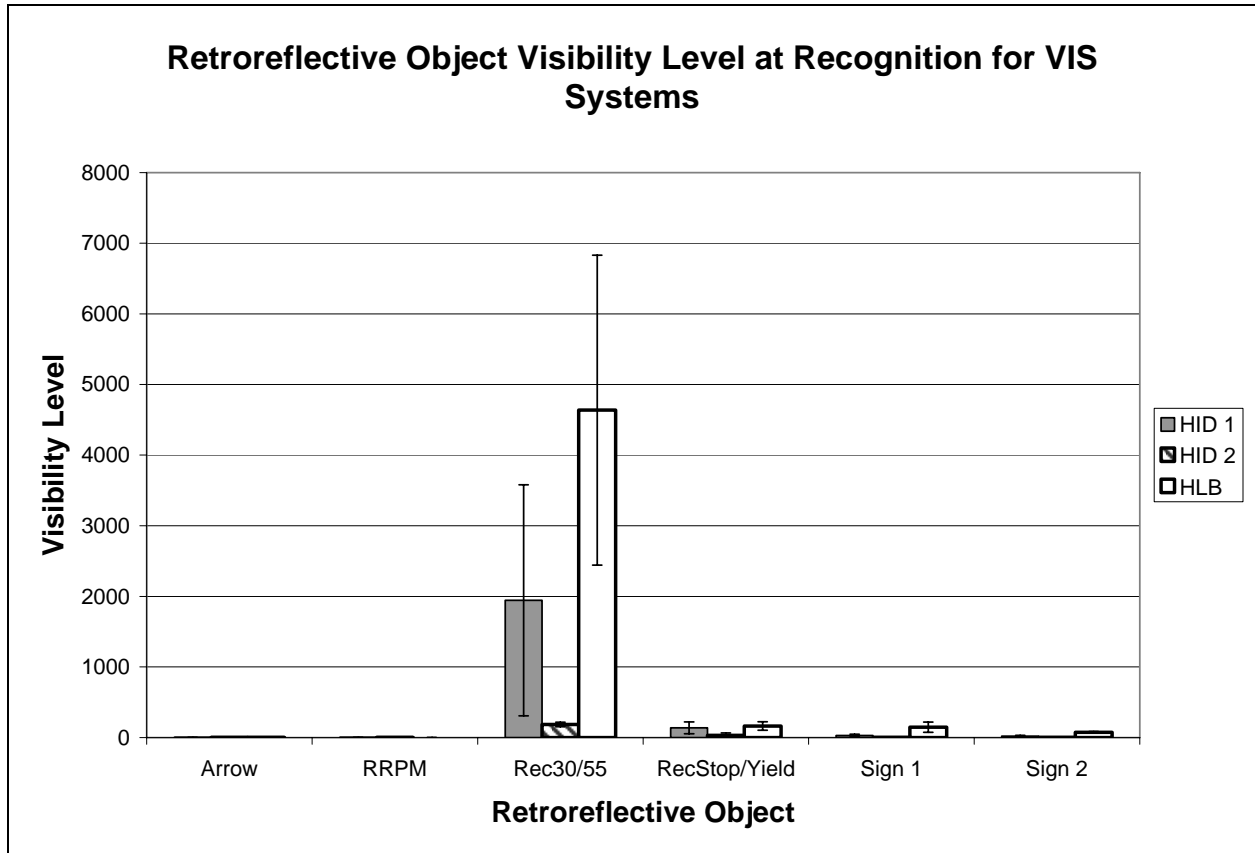


Figure 54. Bar graph. Older driver mean visibility levels at retroreflective object recognition.

One of the difficulties with this comparison is the identification of the visual task. For the calculations, the entire sign was used as the size of the object. For the two sign scenarios, the critical aspects for the recognition tasks were very different; for the two speed limit signs it was the ability to recognize the black letters on the white background, while for yield and stop signs it was the recognition of the triangular shape of a yield sign as compared to the octagonal shape of a stop sign. To effectively use the visibility level for defining human performance, a better definition of the visual task is required.

Photometric Analysis Summary

The performance of the headlamps can be evaluated through photometric analysis. For all of the objects, the HID 2 system provided the lowest measures of photometric performance, even though it had the shortest measurement distances. The beam pattern of the headlamps influenced the results for many of the objects, especially the signs, tire, and dog. The headlamp beam cutoff limited the visibility of the pedestrians by providing uneven luminance as the vehicle approached.

IR SYSTEM USAGE

The photometric information is useful in determining when an IR system appears to be used by the driver for object detection. The following photometric analysis compares the results for the various VESs that incorporated an IR system to the results for the VESs that were visual headlamps only, using object visibility level. If the visibility level of an object at detection by an IR system was less than the visibility level required for detection by the visual VESs, then it was assumed that the IR system's display was used to detect the object.

The visibility level was chosen for this comparison because it is a model that represents the VESs. There are difficulties with the visibility model as discussed earlier, but these difficulties are limited to each of the objects; therefore, the comparison is believed to be valid.

As with the review of the photometric data, this comparison was performed by object group, and it included all of the objects. Only the detection values were considered, except for the recognition of the 30- and 55-mi/h signs and the stop and yield signs.

To assist in the discussions, table 8 outlines the performance of the IR systems in the IR Clear study.

Table 8. IR systems corresponding to minimum and maximum IR distances for detection and recognition.

| Object | Min Detection | Max Detection | Min Recognition | Max Recognition |
|----------------|----------------------|----------------------|------------------------|------------------------|
| Arrow | FIR | NIR 1 | FIR | NIR 1 |
| BlackLF | NIR 2 | FIR | NIR 2 | FIR |
| BlackRT | NIR 2 | FIR | NIR 2 | FIR |
| BloomLF | NIR 2 | FIR | NIR 2 | FIR |
| BloomRT | NIR 2 | FIR | NIR 2 | FIR |
| BlueLF | NIR 2 | FIR | NIR 2 | FIR |
| BlueRT | NIR 2 | FIR | NIR 2 | FIR |
| Dog | NIR 2 | FIR | NIR 2 | FIR |
| FOALT | NIR 2 | FIR | NIR 2 | FIR |
| FOART | NIR 2 | FIR | NIR 2 | FIR |
| LFtrnLF | FIR | NIR 1 | FIR | NIR 1 |
| LFtrnRT | NIR 2 | FIR | NIR 2 | NIR 1 |
| Rec 30/55 | | | FIR | NIR 2 |
| Rec Stop/Yield | | | FIR | NIR 2 |
| RRPM | FIR | NIR 1 | FIR | NIR 1 |
| RTtrnLF | NIR 2 | FIR | NIR 2 | FIR |
| RTtrnRT | NIR 2 | NIR 1 | NIR 2 | NIR 1 |
| Sign 1 | FIR | NIR 1 | FIR | NIR 1 |
| Sign 2 | FIR | NIR 1 | FIR | NIR 1 |
| Tire | NIR 2 | FIR | NIR 2 | FIR |

IR System Usage for Pedestrian Objects

The pedestrian object group included 12 different pedestrian objects. Results of the comparison for this object group are shown in figure 55. For this group, the visibility level of each of the IR systems is significantly lower than that of the VIS systems for every object except the left turn pedestrian on the left. For most objects with IR systems, the visibility level is less than 1, indicating that the actual contrast was below the threshold contrast and that the object was not visually detectable by the participant.

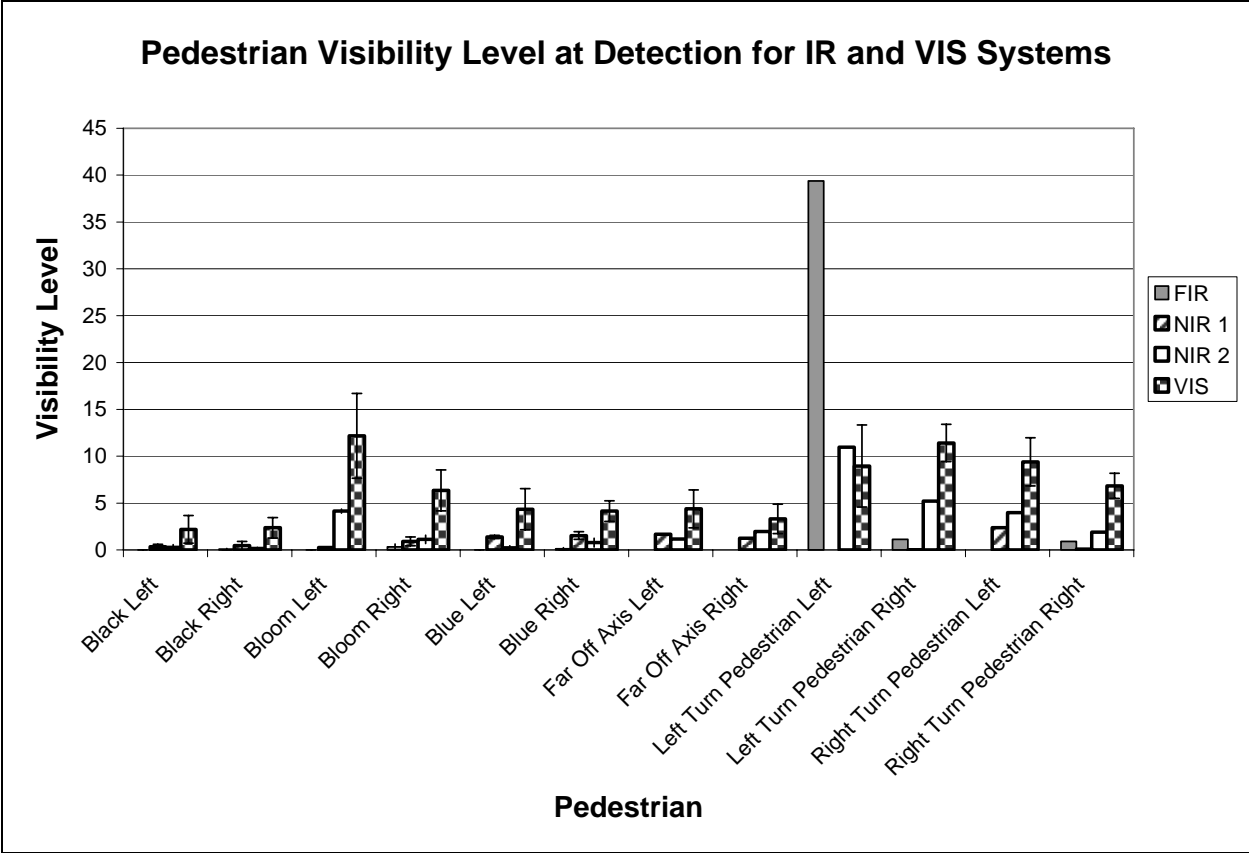


Figure 55. Bar graph. Comparison of older driver mean visibility levels at pedestrian object detection with the IR system versus the VIS systems.

For the left turn left pedestrian, the visibility level at detection with NIR 2 and FIR was higher than with VIS systems, indicating that the NIR 2 and FIR displays did not provide a benefit and were likely not used in this scenario. The visibility level with the NIR 1 system, however, indicates that participants did use this system for detection of the left turn left pedestrian, resulting in longer detection and recognition distances (see table 7). This may have been because of the wider FOV of the NIR 1 display compared to FIR and NIR 2 displays.

The expectation is that the threshold visibility level for an IR system that was not used would be similar to the VIS system performance; however, the threshold visibility level for the FIR and NIR 2 systems was significantly different from that of the VIS systems, indicating that the presence of the IR system distracted the driver and required the object to be significantly brighter to draw attention.

IR System Usage for Obstacle Objects

The obstacle object group for the IR experiments included the dog and tire. The comparison of the visibility level results is shown in figure 56. In this case, it appears that the FIR system probably was used to detect the dog, but the two NIR systems were not. Conversely, the two NIR systems appeared to have been used for the tire tread, but the FIR system was not.

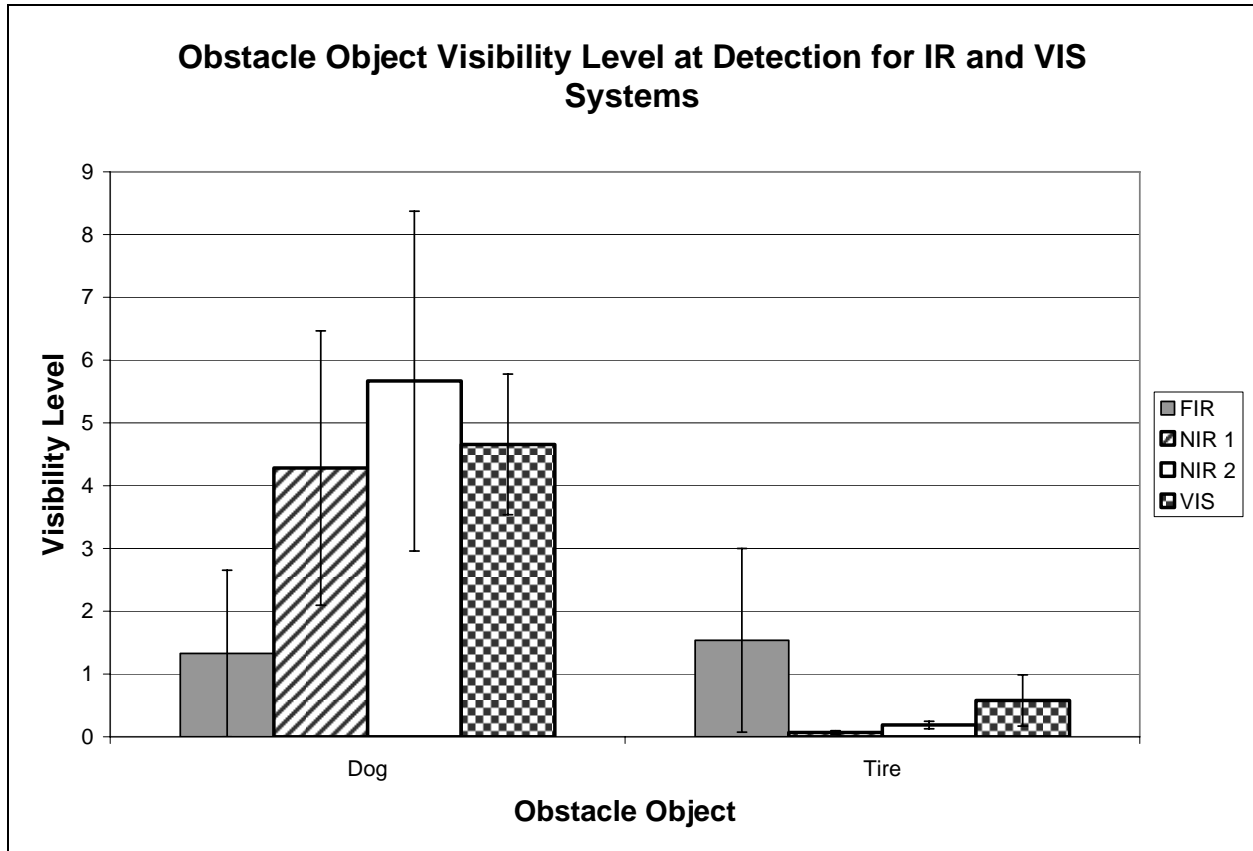


Figure 56. Bar graph. Comparison of older driver mean visibility levels at obstacle object detection with the IR systems versus the VIS systems.

Figure 56 shows that the FIR system was used at all stations to detect the dog, suggesting that the FIR system allowed earlier detection of the dog. Because the dog was heated, it was thermally different than the ambient air, which would have made it detectable with the FIR system.

Neither NIR system was used to detect the dog, which was very small compared to a pedestrian. Its size may have made it difficult to see in the NIR displays. The size is less of an issue for the

FIR system because the dog's thermal system heated not only the dog but also the atmosphere around it, increasing the effective size of the object in the display.

Results indicate participants did not use the FIR system when approaching the tire tread, but they did use the NIR systems. As mentioned, the FIR system relies on a thermal difference between the object and its surrounding environment for detection. Because the tire tread was unheated, it did not provide a thermal difference, and therefore, it was not detectable with the FIR system. For this object, as with the left turn pedestrian object, the system was a distraction, as was indicated by the object's higher visibility level at detection with FIR than with the VIS systems.

IR System Usage for Retroreflective Objects

The retroreflective object group included four different roadway markings and signs. In addition, there were the tasks of recognizing the numbers on the speed limit signs and differentiating between the stop and yield signs. The comparisons of system performances for this object group are shown in figure 57. From this comparison, it is apparent that participants did not use the IR systems for detecting the turn arrow or the RRPM. It appears that for detection of the two signs, participants used the FIR and NIR 2 systems, but not the NIR 1 system.

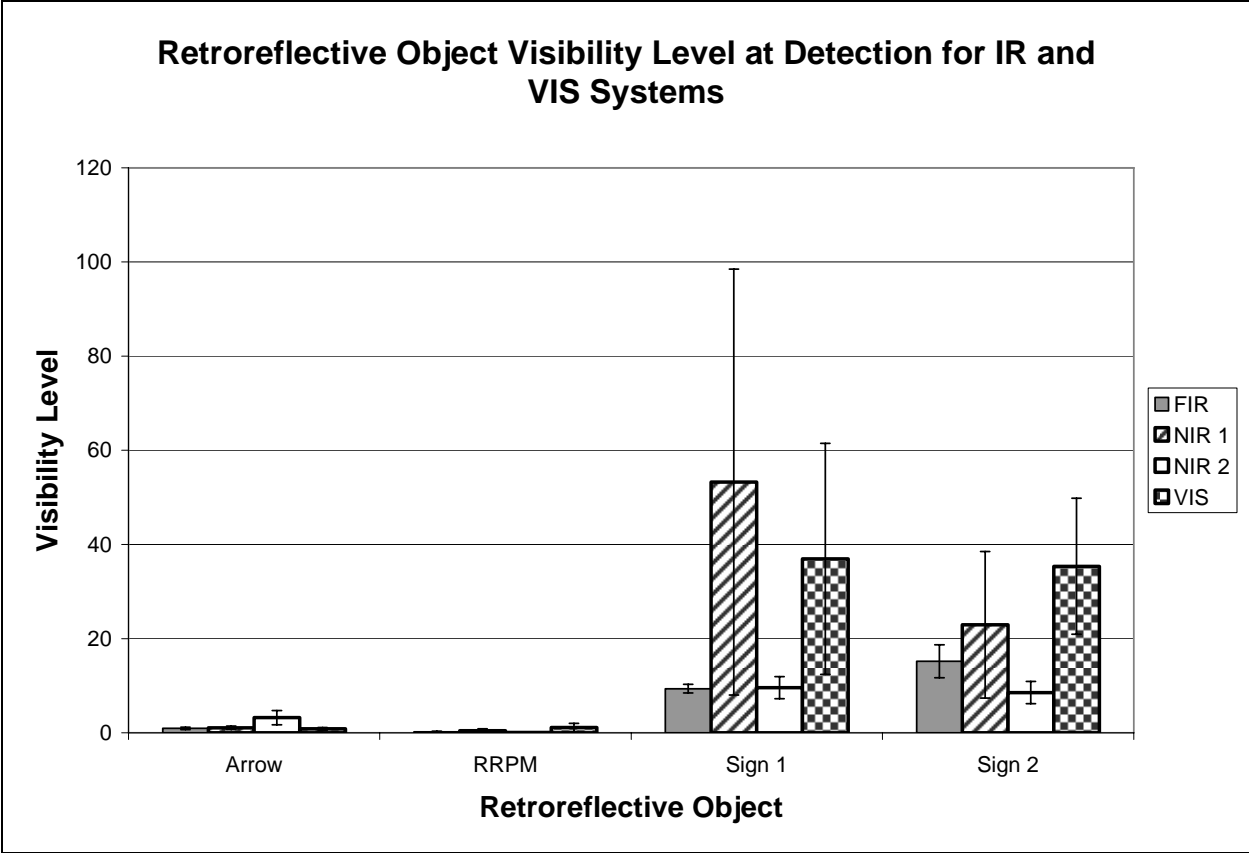


Figure 57. Bar graph. Comparison of older driver mean visibility levels at retroreflective object detection with the IR systems versus the VIS systems.

Signs are designed to reflect visible light back in the direction of the light source. As a vehicle approaches a sign, the light from the headlamps is reflected back even from very long distances, allowing the driver to detect the sign at those long distances. With the two NIR systems, two different emitters were used to provide the IR emission to the roadway. NIR 1 used a laser, which may not be reflected back as efficiently as the broadband emitters used by the NIR 2 system. The NIR 2 emitters provide wavelengths closer to the visual spectrum, and the signs' retroreflective performance may be more efficient at this wavelength range than that of the laser used by NIR 1. This may explain the use of NIR 2 in detection of the signs and the apparent disuse of NIR 1 for this task.

The use of FIR in this scenario might be explained by the temperature gradient of the signs during the IR experiments. The metal signs had a lower thermal resistance than the other objects did, which would have made the signs colder than the atmosphere. The FIR may have detected this temperature difference, making the signs visible in the FIR display.

The results for the IR systems performance for the sign recognition tasks are presented in figure 58. The results indicate the IR systems may have been used to recognize the 30- and 55-mi/h signs but not the stop and yield signs.

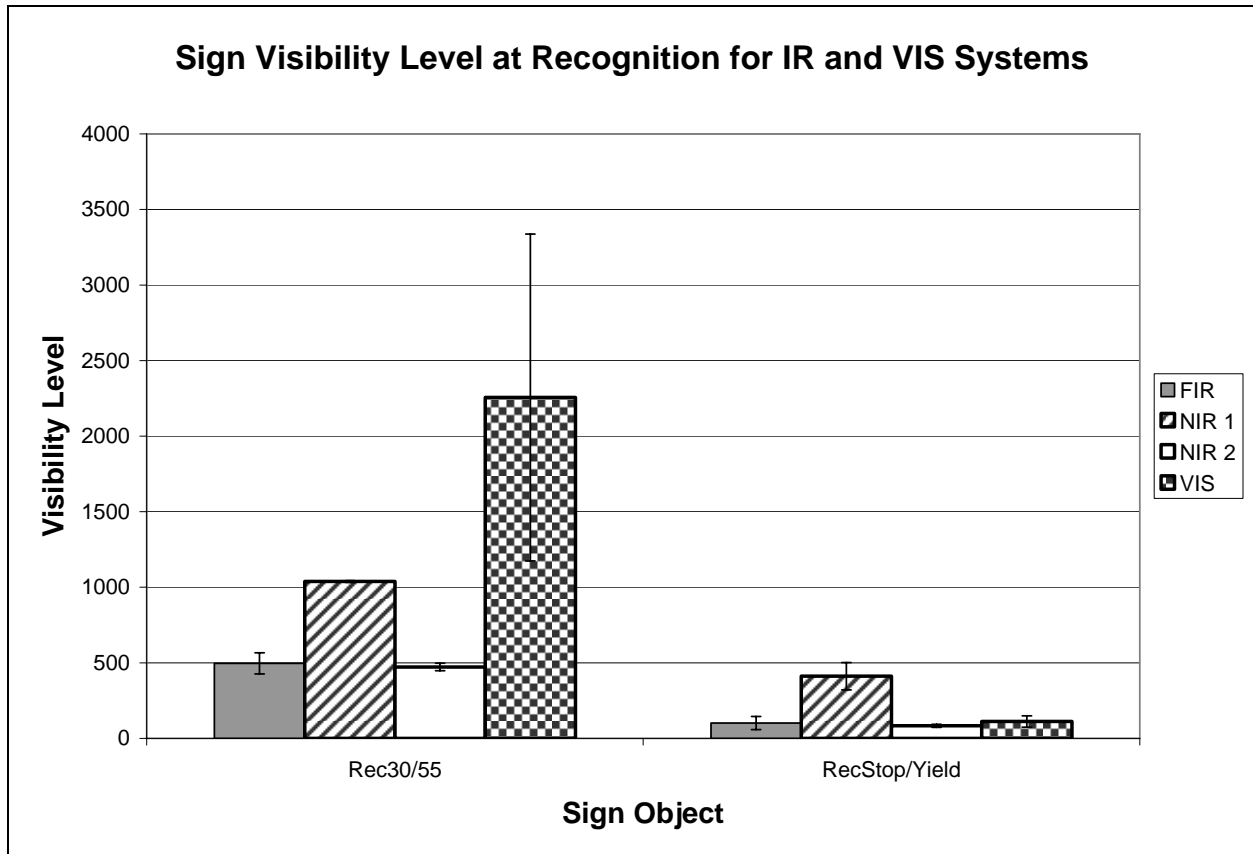


Figure 58. Bar graph. Comparison of older driver mean visibility levels at sign recognition for the IR systems versus the VIS systems.

It is not clear from these results why one sign type could be recognized using the IR systems and the other could not. This task required reading numbers on the speed limit signs and recognizing the shapes of the stop and yield signs. It would be expected that the IR reflectance of the sign material would be the same regardless of the color; the thermal performance of the sign material should also be the same; therefore, a difference was not expected in this comparison.

Two possible reasons for this usage difference exist. The first is that the performance of the headlamps varied widely and may have affected the means of the VIS systems. The second is that the system allowed participants to follow the position of the sign on the roadway accurately

as they approached, thus allowing them to identify the sign type earlier than the VIS systems allowed.

IR System Usage Summary

The comparison of the IR system photometry to that of the visible system photometry allowed for the development of an estimate of the IR system usage. This system usage indicated that the systems were used for all of the pedestrian objects except the left turn pedestrian on the left side of the road, who appeared to be outside of the NIR 2 and FIR systems' FOV. The data indicated that the NIR 2 and FIR systems were a distraction to the driver for that scenario, requiring a higher level of object visibility for object detection than was required for the NIR 1 and visual VESs. The FIR system was used generally for objects that created heat, and the NIR systems generally had difficulties with the smaller objects. The differences in the IR spectral reflectance of some of the objects may also have influenced the near IR system usage.

AGE ANALYSIS

The final aspect of the data comparison is the effect of age. The visibility level model provides an age factor, which accounts for degradation of visual capabilities as a person ages. An age-based comparison of VIS systems and IR systems used the percentage of performance degradation between middle-aged and older drivers as compared to younger drivers. The younger drivers represented 100 percent. These values then were compared to the age factor as specified in the visibility level model. In this comparison, the ages of 30, 50, and 70 were used to represent the age groups. The result of the comparison is shown figure 59.

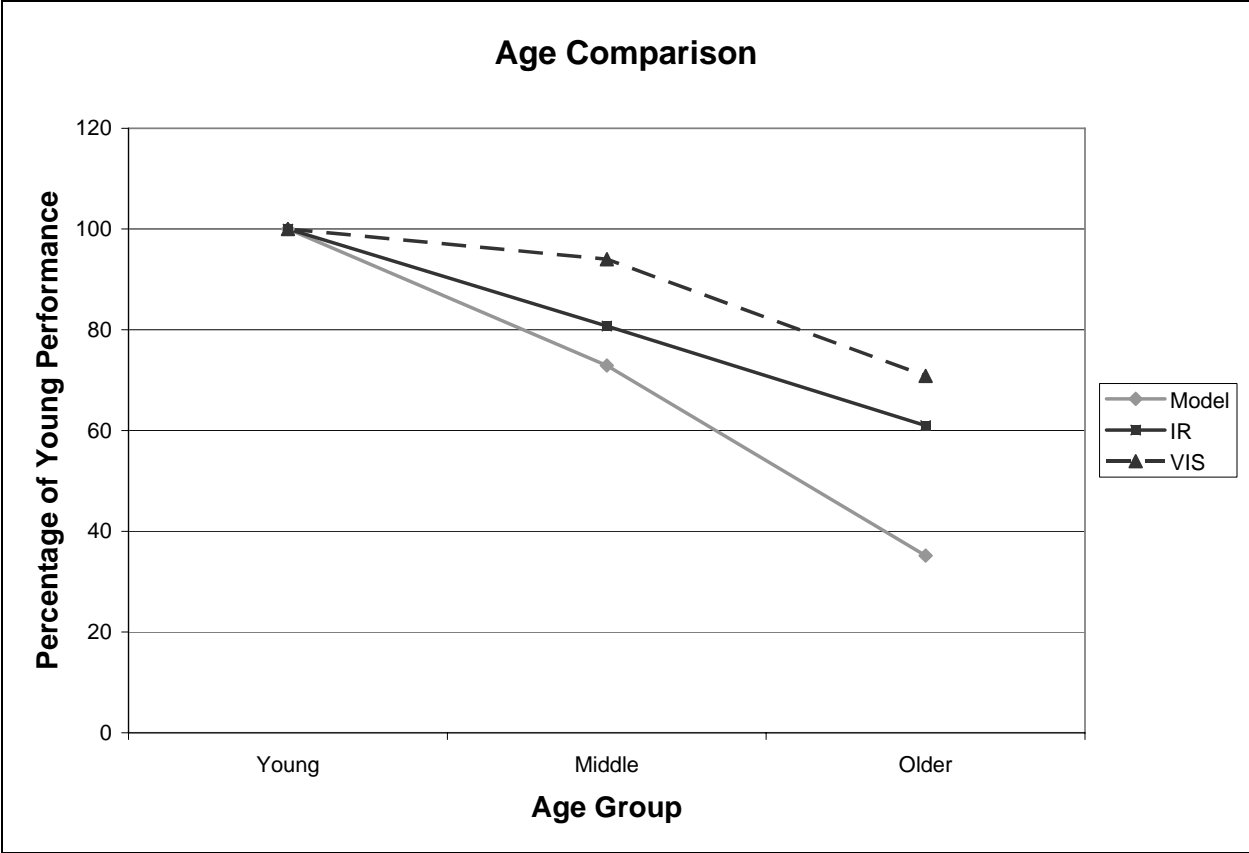


Figure 59. Line graph. Age comparison for detection of pedestrians.

This comparison is based on the detection of the pedestrian objects group. The line graph in figure 59 shows that the age model overestimates the degradation of performance by older drivers. Because this model accounts for changes in the visual system only, it does not allow for improved driver performance with experience that may compensate for the loss of visual capabilities. This may explain the difference between actual performance and the model.

The other interesting aspect of this comparison is the increased degradation in performance with the IR systems as compared to VIS systems. This may indicate that older drivers had greater difficulty adapting to the new IR systems than to changes in the headlamp system characteristics.

CHAPTER 4—DISCUSSION

The research questions posed at the beginning of the project serve as the basis for the discussion of the results. Each of the questions is considered individually.

Is there a relationship between measured data or calculated values and the visibility distance?

After a review of the data measured, it was found that there was a relationship of object luminance to detection distances. This is to be expected because the inverse square law states that the illuminance of an object varies with the square of the distance. Because the luminance is a direct result of the illuminance, the distance relationship holds. The background luminance, contrast, and visibility level did not seem to have the same relationship with distance.

Because all of the photometric measurements are made at threshold of visibility, is the resulting contrast or visibility level the same?

Though the measurements were made at the threshold of visibility, the photometric and physical properties of the objects influenced their resulting contrast and visibility levels. In addition, the position of the object on the road and the location of objects also resulted in different contrast and visibility levels.

Difficulties with the calculation of the visibility level were highlighted. These included the size of the object and the nonuniformity of the object luminance. Further work is required to relate the visual stimulus to the models in a nonuniform environment.

When does an IR system appear to be used by the driver?

Results have shown that drivers often used the IR systems to detect road objects. The systems were used for all of the pedestrian objects except the left turn pedestrian on the left. This object appeared outside of the FOV of the IR systems. The usability of the IR systems for detection of obstacle objects seemed to depend on the object's size and its thermal properties. Finally, the IR systems were used sporadically with the retroreflective objects.

Does having an IR system in the vehicle require higher object contrast and visibility levels at threshold than when the system is not used?

It appears that when an IR system was present but not used, the object visibility level required for detection was either similar to or higher than the visibility level when VIS systems were used. This was particularly evident with the FIR system, which seemed to distract the driver.

What is the effect of beam pattern on the visibility of the objects?

Both the measured and calculated values showed differences between the various VIS systems. Headlamps with narrower beam patterns had longer recognition distances, and they increased visibility levels for road objects. The wider beam patterns provided a higher background luminance. This was particularly evident for the obstacle objects that were close to the road surface.

REFERENCES

1. Calderas, J., personal communication, August 22, 2000.
2. Erion, J., personal communication, June 5, 2000.
3. Dutke, F.F., personal communication, June 20, 2000.
4. Schnell, T., personal communication, August 24, 2000.
5. Adrian, W.K. (1989). "Visibility of Targets: Model for Calculation." *Lighting Research and Technology*, 21(4), 181–188.
6. Illuminating Engineering Society of North America. (2000). *American National Standard Practice for Roadway Lighting: RP-8-00*. New York: Author.

